UNIVERSITI MALAYSIA PAHANG

BORANG PENGESAHAN STATUS TESIS

JUDUL : COMPUTATIONAL FLUID DYNAMICS OF FLOODING, LOADING AND FULLY DISPERSED REGIME IN GAS-LIQUID STIRRED TANK

SESI PENGAJIAN : 2011/2012

Saya **NURUL AIDA BT JAMALUDDIN**
(HURUF BESAR)

mengaku membenarkan tesis (PSM/~~Sarjana~~/~~Doktor Falsafah~~)* ini disimpan di Perpustakaan Universiti Malaysia Pahang dengan syarat-syarat kegunaan seperti berikut :

1. Tesis adalah hakmilik Universiti Malaysia Pahang
2. Perpustakaan Universiti Malaysia Pahang dibenarkan membuat salinan untuk tujuan pengajian sahaja.
3. Perpustakaan dibenarkan membuat salinan tesis ini sebagai bahan pertukaran antara institusi pengajian tinggi.
4. **Sila tandakan (√)

- [ ] SULIT (Mengandungi maklumat yang berdarjah keselamatan atau kepentingan Malaysia seperti yang termaktub di dalam AKTA RAHSIA RASMI 1972)
- [ ] TERHAD (Mengandungi maklumat TERHAD yang telah ditentukan oleh organisasi/badan di mana penyelidikan dijalankan)
- [√] TIDAK TERHAD

Disahkan oleh

(TANDATANGAN PENULIS) (TANDATANGAN PENYELIA)

Alamat Tetap: 101, Jalan Gigih 4,
Taman Sri Lambak,
86000 Kluang,
Johor Darul Takzim.

DR. JOLIUS GIMBUN
Nama Penyelia

Tarikh: January 2012

Tarikh: January 2012

CATATAN:* Potong yang tidak berkenaan.

** Jika tesis ini **SULIT** atau **TERHAD**, sila lampirkan surat daripada pihak berkuasa/organisasiberkenaan dengan menyatakan sekali sebab dan tempoh tesis ini perlu dikelaskan sebagai **SULIT** atau **TERHAD**.

♦ Tesis dimaksudkan sebagai tesis bagi Ijazah Doktor Falsafah dan Sarjana secara penyelidikan, atau disertasi bagi pengajian secara kerja kursus dan penyelidikan, atau Laporan Projek Sarjana Muda (PSM).

SUPERVISOR'S DECLARATION

I hereby declare that I have checked this project and in my opinion, this project is adequate in terms of scope and quality for the award of the degree of Bachelor of Chemical Engineering.

Signature :

Supervisor: DR. JOLIUS GIMBUN

Date : 18 JANUARY 2012

COMPUTATIONAL FLUID DYNAMICS OF FLOODING, LOADING AND FULLY DISPERSED REGIME IN GAS-LIQUID STIRRED TANK

NURUL AIDA BT JAMALUDDIN

Report submitted partial fulfilment of requirements
For the award of the degree of
Bachelor of Chemical Engineering

Faculty of Chemical & Natural Resources Engineering
UNIVERSITI MALAYSIA PAHANG

JANUARY 2012

STUDENT'S DECLARATION

I hereby declare that the work in this project entitled "Computational Fluid Dynamics of Flooding, Loading and Fully Dispersed Regime in Gas-Liquid Stirred Tank" is my own except for quotations and summaries which have been duly acknowledged. This project has not been accepted for any degree and is not concurrently submitted for award of other degree.

Signature :
Name : NURUL AIDA BT JAMALUDDIN
ID Number: KA08021
Date : 18 JANUARY 2012

Dedicated to my supervisor, parents and fellow friends
for all your care, support and believe in me

ACKNOWLEDGEMENTS

I am grateful and would like to express my sincere gratitude to my supervisor Dr. Jolius Gimbun for his superb idea, valuable guidance, continuous encouragement and continuous support for making this research possible. He has always impressed me with his outstanding professional conduct and I am appreciate his consistent support from the first day I applied for this research. I am truly grateful for his tolerance of my naïve mistake and his commitment to my future career. Thanks for the time he spent proofreading and correcting my many mistakes.

My sincere thanks go to all my members and staff of Chemical Engineering Laboratory, UMP who helped me many ways. Many special thanks go to member engine research group for their co-operation, inspirations and support during this study.

I acknowledge my sincere indebtedness and gratitude to my parents for their love, dream and sacrifice throughout my study. Your love, patience and sacrifice have made this dreams come true.

ABSTRACT

The main aim of this work is to perform computational fluid dynamics on gas-liquid stirred tank operating under flooding, loading and fully dispersed regime. This computational method was conducting with the combination of computational fluid dynamics (CFD) and drag model changes by using standard FLUENT model. This current work was attempted to predict the gas hold-up and gassed power number similarly like the result obtained by Ford et al. (2008). The overall research methodology consists of two main steps. First step is about drawing the gas-liquid stirred tank geometric and set the set-up and for the second step is about analysis the flow in gas-liquid stirred tank. After the boundary and the tank geometry have been set up, the selected mathematical model were employed; in the multiphase model, Eulerian-Eulerian model has been used while in turbulence model, two-phase standard k-ε has been employed. Besides that, the drag model of bubble by Schiller & Naumann (1935) was carried out. Diameter of bubbles is taken into account by employed the equation of *Sauter* mean diameter proposed by Calderbank (1958). The gassed power number and gas hold-up inside gas-liquid stirred tank were found to be in fair agreement to the experimental data adopted from Ford et al. (2008). The advantages of this computational method are the operating cost is lower compared to experimental method and besides, it can reduce the time taken to evaluate the performance of gas-liquid STR by neglecting the prototype's design. Through this study, CFD model may be useful to eliminate the impeller flooding in gas-liquid STR.

Keywords: CFD; gas-liquid; Hold-up; gassed power number; flooding

ABSTRAK

Tujuan utama kerja ini adalah untuk melaksanakan pengiraan dinamik bendalir (*Computational Fluid Dynamics, CFD*) pada gas-cecair dikacau di dalam tangki yang beroperasi di bawah kawasan banjir, pemuatan dan sepenuhnya bersurai. Kaedah pengiraan ini telah menjalankan dengan kombinasi dinamik bendalir pengiraan (*CFD*) dan seret perubahan model dengan menggunakan model FLUENT standard. Semasa kerja ini, ia cuba meramalkan gas memegang dan kuasa nombor gas yang sama seperti keputusan yang diperolehi oleh Ford et al. (2008). Metodologi penyelidikan keseluruhan terdiri daripada dua langkah utama. Langkah pertama ialah melukis geometri cecair gas dikacau tangki dan menetapkan set-up dan untuk langkah kedua ialah menganalisis aliran cecair gas tangki dikacau. Selepas sempadan dan geometri tangki telah direka, model matematik yang dipilih akan digunapakai dalam model yang berbilang-fasa, model *Euleran-Euleran* telah digunakan semasa dalam model gelora, dua fasa standard k-ε juga telah digunakan. Selain itu, model seretan gelembung oleh Schiller & Naumann (1935) telah dijalankan. Diameter buih diambil kira dengan menggunakan persamaan diameter min Sauter yang dicadangkan oleh Calderbank (1958).Bilangan pengudaraan kuasa dan gas tahan dalam cecair gas dikacau tangki didapati dalam perjanjian yang adil kepada data uji kaji yang diguna pakai dari Ford et al. (2008). Kelebihan kaedah ini pengiraan kos operasi lebih rendah berbanding dengan kaedah eksperimen dan selain itu, ia boleh mengurangkan masa yang diambil untuk menilai prestasi STR gas-cecair dengan mengabaikan reka bentuk prototaip. Melalui kajian ini, model CFD mungkin berguna untuk menghapuskan banjir pendesak dalam STR cecair gas.

Kata kunci: CFD; gas-cecair; gas memegang; bilangan kuasa pengudaraan; banjir

TABLE OF CONTENTS

LIST OF FIGURES

LIST OF TABLES

LIST OFSYMBOLS

a_i	Interfacial area
α	Constant (Eq. 2.12)
α_g	Gas hold up
α_l	Liquid volume fraction
β	Constant (Eq. 2.12)
C	Clearance
C	Dimensionless shape factor (Eq. 2.2)
C_D	Drag coefficient
C_L	Lift coefficient (Eq. 3.3)
$C_{\varepsilon 3}$	Constant equation (Eq.3.14)
D	Tank diameter
d_{32}	*Saute*r mean diameter
d_{bi}	Local bubble diameter
d_{bs}	*Sauter* mean diameter
ε	Energy dissipation
ε_g	Local gas hold up
F_{lg}	Gas flow number
Fr	Froude number
$F_{\beta\alpha}$	Interaction forces between continuous and dispersed phase

$\vec{F}_{lg}$	Interaction force per unit volume
$\vec{F}_{lift,l}$	Lift force
$\vec{F}_{vm,l}$	Virtual mass force
g	Gravitational force
$\vec{g}$	Acceleration due to gravity and
$G_{k,l}$	Rate of production of turbulent kinetic energy
H	Tank height
k_La	Mass transfer coefficient
k	Turbulent kinetic energy
N	Impeller speed
N_{CD}	Impeller speed of completely dispersed
N_F	Impeller speed of flooded
N_R	Impeller speed of recirculation
N_p	Power number
N_{pg}	Gas power number
n_i	Number of particles
$\Pi_{\varepsilon,l}$	Influence of the dispersed phase on continuous phase
P	Power consumption
P_g	Gassed power
P_o	Ungassed power
ρ_l	Liquid density
Q_g	Aeration rate
Re	Reynolds number
R_b	Blade area ratio

T	Tank internal diameter
$\bar{\bar{\tau}}_l$	Liquid phase stress-strain tensor
Γ	Torque
U_g	Superficial gas velocity
μ	Viscosity
$\vec{u}_l$	Liquid velocity
V	Volume
$V\infty$	Bubble rise velocity
v_{sg}	Superficial gas velocity
σ	Interfacial tension

LIST OF ABBREVIATIONS

2D	Two dimensions
3D	Three dimensions
BDM	Bubble density model
CARPT	Computer-automated radioactive particle tracking
CFD	Computational Fluid Dynamics
CT	Computed tomography
DRW	Discrete random walk
EBI	Eddy-bubble interaction
GRT	Gamma Ray Tomography
IO	Inner-outer method
LDA	Laser Doppler Anemometry
LPM	Liter per minute
MRF	Multiple reference frame
PBM	Population balance modelling
PIV	Particle Image Velocity
RANS	Reynold averaged Navier-Stokes
RDT	Rushton turbine
rpm	Rotational per minute
SG	Sliding grid method
SN	Schiller-Naumann drag model

SR	Solidity ratio
STR	Stirred tank
UDF	User defined function

CHAPTER 1

INTRODUCTION

1.1 Motivation

In the process industry, many unit operations are performed in stirred tanks and reactors. There are various fields like building construction; chemical manufacturing and food processing in which mixing tanks manifest themselves and commonly involving the reaction between liquid and gas phases. But, for the successful working in the industry, efficient and proper machinery or equipment are required. The good performance of stirred reactor can be achieved by making adjustment on the inappropriate operating hardware and parameters. The parameters like impeller shapes (Murthy et al., 2008; Sun et al., 2006), impeller speed (Ford et al., 2008; Taghavi et al., 2010; Wang et al., 2006; Qingbai et al., 2010; Ahmed et al., 2010), impeller position (Bakker and Akker, 1994), sparger position (Bakker and Akker, 1994), aeration rate (Bakker and Akker, 1994; Wang et al., 2006), have been studied by them experimentally and numerically. In order to design the highly performance of stirred tank, it is required for engineer to know local gas hold-up which depends on the gas and liquid properties, superficial gas velocity, sparger and impeller design and power consumption and how it changes with different operating conditions (Ford et al., 2008). Flooded is undesirable as it can lower the mass transfer in gas-liquid STR (Bakker & Akker, 1994; Xiao & Takahashi, 2007). While in the loaded regime has poor gas distribution throughout the vessel and completely dispersed regime is highly desirable operating regime due to the gas being completely dispersed at a low power input (Ford et al., 2008).

With the advancement of technology, the flow patterns inside the gas-liquid flow can readily be gained by Computational Fluid Dynamics (CFD) whereby it is not required high in cost and longer time to design the prototype or pilot scale testing compared to experiment set-up. The flow patterns of gas-liquid in STR are complicated to predict and have been studied by many authors by using the CFD (Khopkar and Ranade, 2005; Murthy et al., 2008; Gentric et al., 2005; Deen et al., 2002; Ahmed et al., 2010; Taghavi et al., 2010). Ford et al. (2008) and Heindel et al. (2008) have been used X-ray Computed Tomography to measure the local time-averaged gas hold-up in STR but this equipments is very expensive and cannot measure the different size of gas bubbles that coexist in gas-liquid STR. Nevertheless, other authors also utilized the sophisticated equipments in their experiments to measure the flow pattern in gas-liquid STR like Gamma Ray Tomography, GRT (Veera, 2001; Bukur et al., 1996), Particle Image Velocity, PIV (Deen et al., 2002; Laakonen et al., 2005), Laser Doppler Anemometry, LDA (Rutherford et al., 1996).

1.2 Problem Statement

In process industry, mixing tank is widely used to conduct any process that can contribute an annual turnover value of around €1370 billion worldwide, thus indicate that the importance of stirred tank reactors themselves (Butcher and Eagles, 2002). Poor mixing of stirred tank can be identified by presence of impeller flooding which has low in mass transfer coefficient (k_La). Extensive Experimental methods available to evaluate performance of gas-liquid STR for example Gamma Ray Tomography (GRT), Laser Doppler Anemometry (LDA) and Particle Image Velocity (PIV). However, experiment often expensive to setup due to costly instrument (i.e. PIV, GRT, LDA) and often needs long time to develop a prototype for testing (Gimbun et al., 2009). Alternatively, CFD can be employed to evaluate performance of gas-liquid STR at lower cost and in shorter time. Thus, this work attempts to evaluate gas-liquid STR performance via CFD focusing mainly on the flooding to dispersed regime transition. Therefore, the CFD model developed in this work may be useful to eliminate the impeller flooding.

1.3 Research Objective

The aim of this study is to perform the Computational Fluid Dynamics (CFD) on gas-liquid stirred tank operating under flooding, loaded and fully dispersed regime with the hope the model can be applied in the future to eliminate impeller flooding that can cause poor and inefficient mixing in gas-liquid stirred tank.

1.4 Scope of Research

In order to achieve the objective, this present work was study on gassed power number in gas-liquid stirred tank via CFD at various flow regimes. Besides that, gas hold-up was studied by comparing the prediction studied by Ford et al. (2008) by employed the turbulence model, Eulerian-Eulerian model and drag model for bubble in CFD at various flow regime.

1.5 Significance of Research

By employing CFD simulation in this present work, it can reduce the cost of development and design the gas-liquid stirred tank instead of using the experimental method that required high cost of instruments. Besides that, this simulation can reduce the time taken to evaluate the performance of gas-liquid stirred tank in comparison with the experimental method because it can be a time-consuming in order to design the prototype and pilot scale testing of stirred tank reactors.

1.6 Structure of Thesis

The structure of the reminder of the thesis is outlined as follow:

Chapter 2 provides a description of the applications and general description on the flow characteristics of the system, as well as the dimensionless groups and correlations to account for the flow phenomena are presented. This chapter also provides a summary of the previous study on multiphase flow or single flow via numerical simulation or experimental work. The empirical equations to be used are also presented in this chapter.

Chapter 3 gives a review of the CFD approach applied for stirred tanks modelling gas-liquid flows including the multiphase modelling, drag force modelling, turbulence modelling and impeller modelling. The modelling strategy and the tank dimension were explained briefly in this chapter. The step to conduct this CFD simulation also presented.

Chapter 4 discussed the power consumption and the gas hold-up in gas-liquid stirred tank. The time averaged of the flow was measured at different impeller speed. The result of aeration power, local gas hold-up along *x*-axis and average *z* slice hold-up were compared with predicted result and experimental data from Ford et al. (2008). This chapter also show the flow contour inside the gas-liquid stirred tank.

Chapter 5 draws together a summary of the thesis and outlines the future work which might be derived from the model developed in this work.

CHAPTER 2

LITERATURE REVIEW

2.1 Overview

This chapter will give a brief description on the application of stirred tank in industry. Besides that, the advantages of CFD will be described and further description of three different flow regimes in gas-liquid stirred tank will be discussed. Other than that, the CFD simulation in gas-liquid stirred tank will be further discussed. Moreover, the empirical equations that will be used throughout this study will be described briefly. On the other hand, several published research on the experimental and numerical simulation method of STR will be reviewed clearly.

2.2 Application of Stirred Tank

Many chemical productions used stirred tank in process industry. They are required for carrying out any process efficiently and conveniently. It is validated with the studied made by Butcher and Eagles (2002), saying that about 50% chemical process taking place in stirred tanks and give $1290 billion per year of profit income. This indicates that the importance of gas-liquid stirred tank in variety of chemical process such as hydrogenation, oxidation, chlorination and aerobic fermentation. Therefore, some examples of such process will be described below.

2.2.1 Hydrogenation

Hydrogenation process is widely applied in industry for instance pharmaceutical, petrochemical and food processing. The normal process conditions of this process involve elevated pressure and temperature in the presence of a precious metal catalyst (i.e nickel for margarine production). One example of food processing that used hydrogenation process is producing margarine or butter from a certain fatty oils; vegetables or animals. In this production, hydrogen is sparged into the bottom of the tank and will react with the carbon-carbon double bond inside the tank. The reaction is simplified as below:

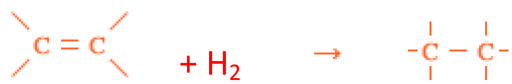

$$CH_2 = CH_2 + H_2 \xrightarrow{Ni} CH_3 - CH_3$$

Figure 2.1: Hydrogenation reaction

2.2.2 Aerobic Fermentation

For aerobic fermentation, oxygen transfer is a key variable and is a function of aeration and agitation (Potumarthi et al., 2007). This kind of process is commonly used in food and pharmaceuticals industries. Some examples of the product consist of protease enzyme (Kumar and Hiroshi, 1999), bacteria (Boodhoo et al., 2010), yeast and vitamin. The main feature of aerobic fermentation is the provision for adequate aeration; in some cases, the amount of air needed per hour is about 60-times the medium volume. Therefore, stirred tank used for aerobic fermentation have a provision for adequate supply of sterile air, which is generally sparged into the medium.

2.2.3 Wastewater Treatment

In wastewater treatment process, mixing tank is used to keep and mix the sludge. This is due to maintaining the sludge conditions from being septic. Therefore, sludge should be keep mixing, aerobic conditions (adequate air) must have maintained and chemicals need to be applied into the mixing tank in order to eliminate septicity and reduce odour potential in mixing tanks. The amount of air needed to mix the full tank volume is depends on the sludge.

2.2.4 Oxidation

Oxidation process is widely in biological process that involved the microorganism. One example of such process carried out in aerated stirred tanks has been reported by Gomez and Cantero (2002). They reported that *Thiobacillus ferrooxidans* is an acidophilic bacterium that has the ability to oxidise ferrous to ferric iron in the presence of atmospheric oxygen and carbon dioxide and it is a dominant organism in the process of value metal extraction by microbial leaching of pyritic ores. Hence, the main purpose for the air sparging into stirred tank is to stimulate growth of bacteria (oxygen is required for respiration) for bioleaching process.

2.3 Flow Regime in Gas-Liquid Stirred Tank

Gas-liquid stirred tank is widely used in process industry to carry out reaction between gases and liquids. The flow patterns inside stirred tank are complicated and can be classified into four which are flooded, loaded, fully dispersed and gas recirculation. This part has been studied by many authors (Myers et al., 1994; Bombac and Zun, 2006; Ranade et al., 2008; Ford et al., 2008). Further description on the four class of flow regime will be described below. The pictures of different bulk flow pattern taken by Ford et al. (2008) can be seen at **Figure 2.2, Figure 2.4, Figure 2.5.**

2.3.1 Flooded Regime

Flooded is highly undesirable in any process involve in gas-liquid stirred tank. In the presence of flooding in gas-liquid stirred tank can effect the performance of mixing because of the cavity formation behind the impeller blades. Therefore, this present work was carried out in CFD model in order to eliminate the impeller flooding. Flooding occurs when the impeller speed is low ($0 < N < N_f$) and gas flow rates are high which gas flow number and gassed power number are high. These leads to low gas hold-up and low mass transfer rates (Ford et al., 2008). According to Khopkar et al. (2005), as the vertical distance increase from impeller region, the gas hold-up will be increase due to the decreasing of pressure acting on the bubble and also decreasing of bubble rise velocity. Ford et al. (2008) have been captured the flow pattern as flooded by using X-ray Computed Tomography as shown in **Figure 2.2**. They reported that *x*-slice compares well with the accompanying visible light picture, which also shows the large bubble size for these conditions. There are very few bubbles near the tank walls, which is common of the flooded region.

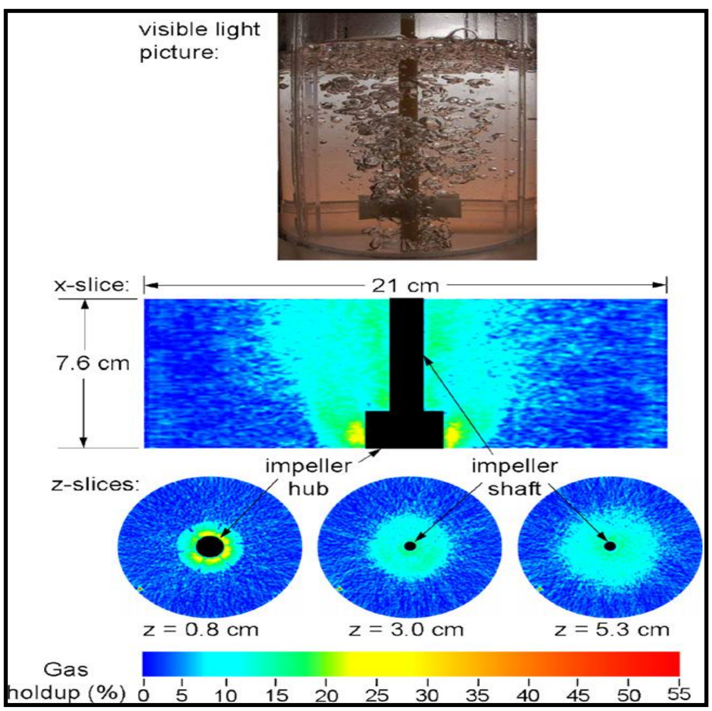

Figure 2.2: Flooded flow regime at Q_g = 9LPM and N = 200 rpm (Ford et al., 2008)

2.3.2 Loaded Regime

Loaded regime occurred as the flow transitions from flooded. Loaded pattern can be identified when the impeller speed is higher than impeller speed of flooded as well as lower than impeller speed of completely dispersed ($N_f < N < N_{cd}$). The flow regime in stirred-tank reactors is strictly linked to the gas cavity structure developed behind the blades (**Figure 2.3**). The differences occurring in the cavity structure have been excellently described by Nienow et al. (1985). According to Ford et al. (2008), loaded regime is still poor gas distribution due to the buoyant forces of the gas being larger than the radial drag force resulting from the liquids mixing even the impeller at this regime is better able to radially distribute the gas. Besides that, across the transitions of flooded to loaded, the bubbles have decreased in size and are located throughout a larger region of the stirred tank as shown by visible light picture (**Figure 2.4**). In fact there a very few bubbles below the impeller as well as defined as the characteristics of loaded.

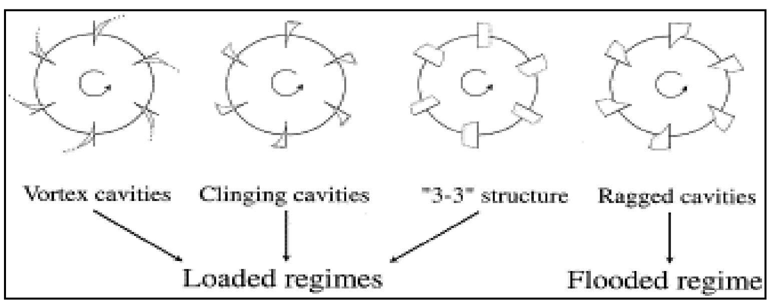

Figure 2.3: Cavity structure at loaded and flooded regime

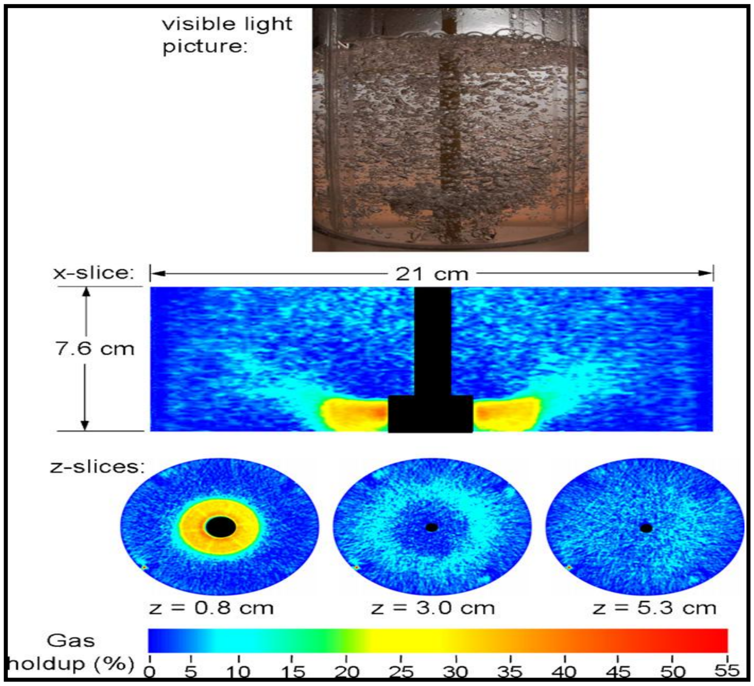

Figure 2.4: Loaded flow regime at Q_g = 9LPM and N = 350 rpm (Ford et al., 2008)

2.3.3 Fully Dispersed Regime

Fully dispersed regime or completely dispersed regime is highly desirable operating regime due to the gas being completely dispersed in at lower power input. If ($N_{cd} < N < N_r$), the flow is falls into the fully dispersed regime due to the increased of impeller's angular velocity. As reported by Ford et al. (2008), the CT images show high gas holdups throughout the entire imaging region, which are higher than those for the other two conditions; flooded and loaded. As shown by the visible light picture (**Figure 2.5**), bubbles have further decreased in size and they are located throughout the stirred tank. If the impeller speed is increased still further, gas recirculation can be observed ($N = N_r$) (Paglianti et al., 2000).

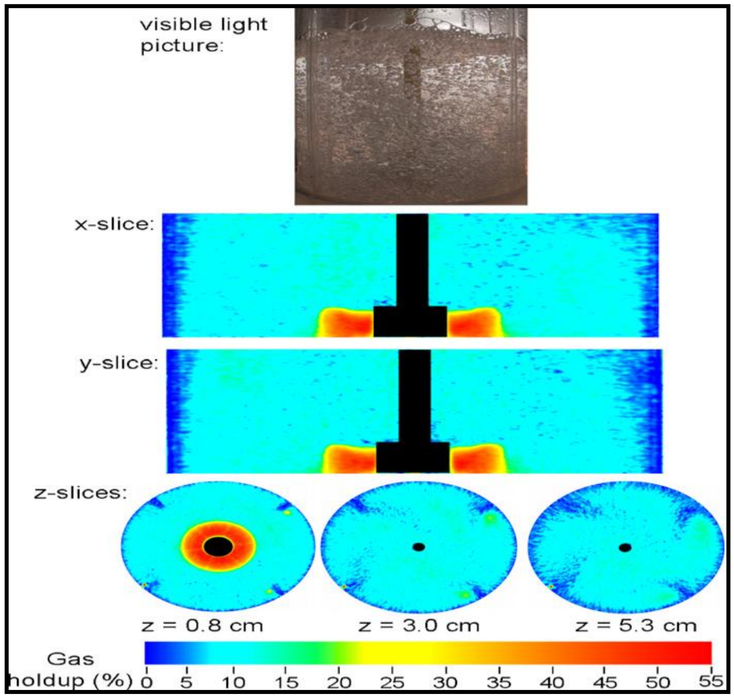

Figure 2.5: Completely dispersed flow regime at Q_g = 9LPM, N = 700 rpm

(Ford et al., 2008)

2.4 CFD Simulation

The CFD simulation is used to portray hydrodynamics behaviour in the reactor, including the velocity field, biogas volume fraction, turbulence kinetic energy and shear strain rate. Due to the progress in computer technology CFD seems now able to deal with industrial applications at moderate costs and turnaround times. The future relevance of CFD will therefore depend on how accurate complex flows can be calculated. Since many flows of engineering interest are turbulent, the appropriate treatment of turbulence will be crucial to the success of CFD (Sodja, 2007). Configuration optimization of the reactor is achieved by optimizing the impeller design. In the last two decades, computational fluid dynamics (CFD) has become known as a potential tool for ‘a priori prediction’ of the flow field in the stirred reactors. The CFD based models were shown to be successful in simulating single phase flows generated by a single impeller of any shape in the stirred reactor (Ranade, 2002).

2.5 Empirical Equations for STR

There are a number of equations have been found in order to characterise the performance of stirred tanks. Many researchers have been studied widely by followed the equations based on what they are studied for (Bakker and Akker, 1994; Ranade et al., 2008; Scargiali et al., 2007; Ahmed et al., 2010). Besides, all the equations involved are dimensionless. The power consumption, *P*, of a stirrer is described by the power number, N_P, which depends on fluid properties and on the geometrical parameters of the mixing device. The equation given by:

$$N_p = \frac{P}{\rho N^3 D^5} \tag{2.1}$$

where ρ is the density of the container fluid; *N* is the impeller rotational speed and *D* is the impeller diameter. According to Taghavi et al. (2010), the power number can be related to the Reynolds number, R_e and Froude number as showed by Holland and Bragg (1995) as below:

$$N_P = CRe^x Fr^y N_P \tag{2.2}$$

C is an overall dimensionless shape factor which represents the geometry of the system and Reynolds numbers, *Re* and Froude numbers, *Fr* are:

$$Re = \frac{\rho N D^2}{\mu} \tag{2.3}$$

$$Fr = \frac{N^2 D}{g} \tag{2.4}$$

where ρ is the fluid viscosity and g is the acceleration of gravity. Reynolds number represents the ratio of the inertial to viscous forces and Froude number represents the ratio of inertial to gravitational forces. According to Gimbun et al. (2009), in the fully turbulent region which is Re > 10^4, the power number is normally constant. But in laminar and transitional regimes Re < 10^4, Re is decreasing with the increasing of Reynolds number. All these three equations can be derived from Navier–Stokes equation. In this present work, three different flow regime will be studied by using CFD, hence may be used the gas flow number equation in order to characterize the gas-liquid dispersion in stirred tank. The gas flow number is also called aeration number is given by:

$$F_{lg} = \frac{Q_g}{ND^3} \tag{2.5}$$

where Q_g is the volumetric gas flow rate to the vessel.

Figure 2.6 shows the gas-liquid flow pattern illustrated by Paglianti et al. (2000) across three different regime; flooding, loading and complete dispersed. In section 2.3.1, flooding is highly undesirable situation where the impeller is unable to disperse the aerated gas effectively to the whole tank due to the formation of cavity behind the impeller blades as shown at **Figure 2.3.** This may cause to the rises of gas in a restricted region around the impeller shaft (**Figure 2.6A**). As the impeller speed (N) is increased at constant gas flow rate (Q_g), the gas flow enclosed the entire cross section above the impeller and the impeller is loaded (**Figure 2.6B**). At constant gas volume flow rate, a complete dispersion of the gas (**Figure 2.6C**) can be achieved by increasing the impeller speed.

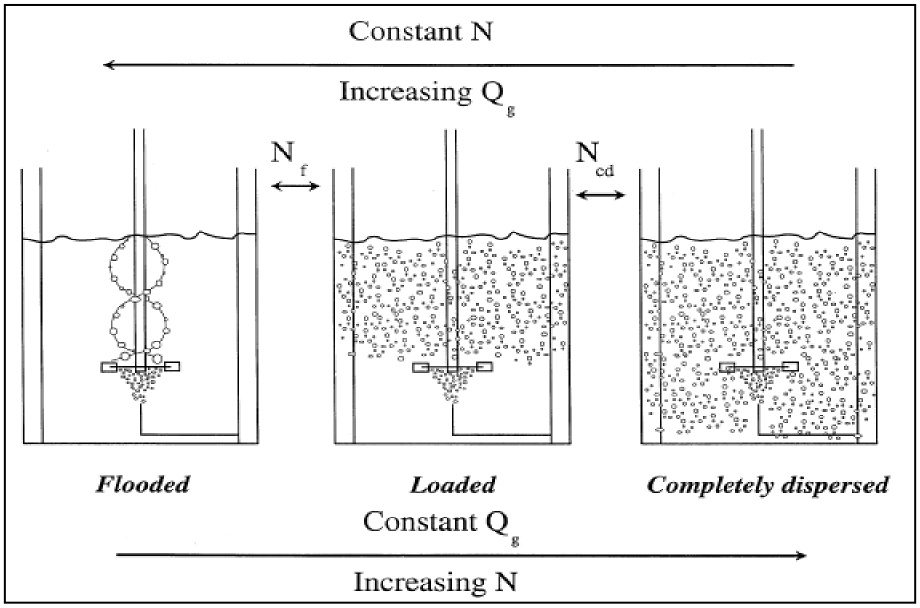

Figure 2.6: Illustration of the gas –liquid flow pattern by Paglianti et al. (2000).

A) Flooded, B) Loaded, C) Complete dispersed

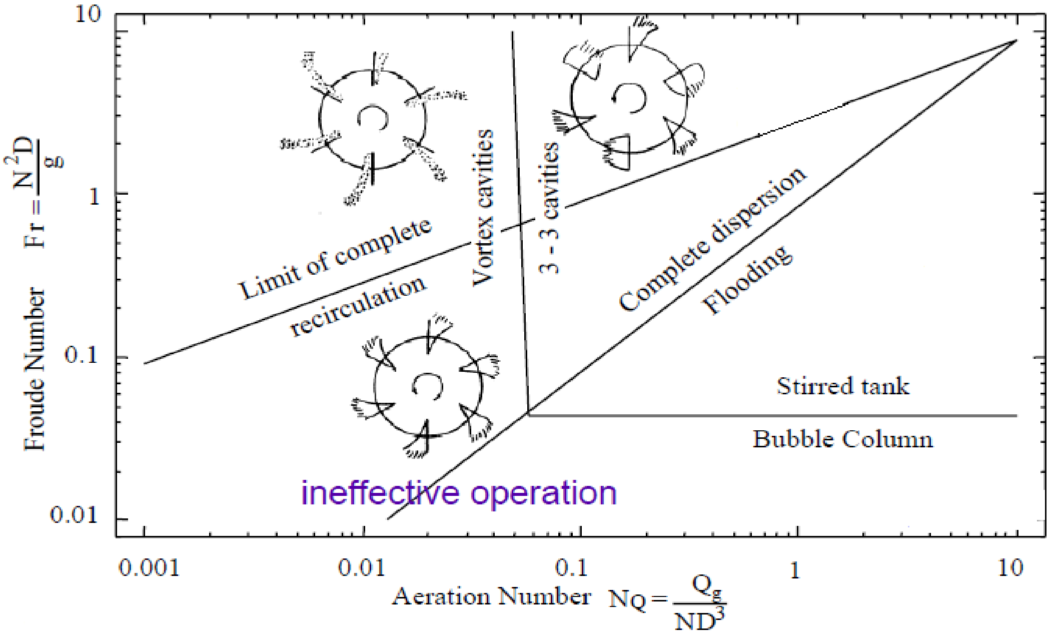

Figure 2.7: Impeller flow regime map (Adapted from Warmoeskerken and Smith, 1985)

Nevertheless, transition between the various flow regimes is much better illustrated by the impeller flow regime maps as shown at **Figure 2.7** illustrated by Warmoeskerken and Smith (1985). Besides that, Bakker et al. (1994b) has formulated the flow regimes map for Rushton turbine and CD-6 impeller using a similar set of equations. The following STR bulk flow regime transitions at constant gas flow rate with increasing impeller speed have been correlated by (Nienow et al., 1985) at too high gas flow, gas dominates the flow and the impeller becomes flooded at an impeller speed N_F .

$$(F_{lg})_F = 30(Fr)_F(\frac{D}{T})^{3.5} \tag{2.6}$$

for $N_F < N < N_{CD}$, the impeller is loaded but the gas is not completely dispersed and correlated by (Nienow et al., 1977):

$$(F_{lg})_{CD} = 0.2(Fr)_{CD}{}^{0.5}(\frac{D}{T})^{0.5} \tag{2.7}$$

for $N_{CD} < N < N_R$, the gas is completely dispersed; and when $N > N_R$, large amounts of gas recirculate throughout the vessel and is described by (Nienow and Wisdom, 1976):

$$\left(F_{lg}\right)_R = 13(Fr)_R^2(\frac{D}{T})^5 \tag{2.8}$$

where $(F_{lg})_i$ and $(Fr)_i$ represent the gas flow number and the corresponding Froude number at flooding, complete dispersion, and recirculation, respectively. For efficient operation, the impeller speed N should be greater than the impeller speed at which complete gas dispersion occurs ($N > N_{CD}$).

Table 1. Solidity ratio, blade area ratio and other variables.

Impeller	*SR*	$R_{b,\perp}$	n_b	*D*(m)	*Po*	Fl_l
A315	90%	77%	4	0.178	0.76	0.74
Leeuwrik	160%	80%	6	0.168	2.55	—
PBT	60%	45%	6	0.176	1.55	0.81

Table 2.1: Solidity ration, blade area ratio and other variables (Bakker and Akker, 1994).

Besides that, Bakker and Akker (1994b) in their studies reported that the projected blade area ratio is not the only parameter affecting the cavity formation and stalling and that these processes will also depend on the shape of the impeller blades. The value for the solidity ratio, R_b and the number of blades are listed in **Table 2.1** together with the impeller power number given by:

$$P_O = \frac{P}{\rho N^3 D^5} \tag{2.9}$$

P is the power consumption for the impeller. Moreover, extensive data for power input in gas–liquid dispersions by a six-bladed disc turbine over a vessel size range of 0.21–3.33 m and superficial gas velocities $U_g \leq 0.053\ ms^{-1}$ were correlated by Hughmark (1980) and presented in the form:

$$\frac{P_g}{P_o} = 0.1\left(\frac{Q_g}{NV}\right)^{-1/4}\left(\frac{N^2 D^4}{g D_i V^{2/3}}\right)^{-1/5} \tag{2.10}$$

Equation above is based on 391 data points with a standard deviation between calculated and experimental values of +11:7% (Kapic et al., 2006). Besides that, power number also can be calculated from the total moments acting on the shaft and impeller wall. This moment also called as torque, (Γ) whereby the equation as followed:

$$P = 2\pi N\Gamma \tag{2.11}$$

where N is the impeller speed.

Stirred tank has been used widely in many industrial process especially chemical and oil production but in order to predict the volumetric mass transfer coefficient (k_La) is extremely difficult. This is due to the complexity of multiphase (gas-liquid) hydrodynamics. According to Kapic et al. (2006), volumetric mass transfer coefficient (k_La) is a function of specific power density (P_g/V) and superficial gas velocity (U_g). k_La was correlated as below:

$$k_La = C_1\left(\frac{P_g}{V}\right)^{\alpha} U_g^B \tag{2.12}$$

where the exponents α and β range from 0.3 to 0.7 and 0 to 1.0 respectively. However, Bakker et al. (1994) used the constant of α and β which is 0.6 that obtained from fitting of experimental measurements. Nevertheless, through Kapic and freinds study, he proposed **eq. (2.13)** in the form of **eq. (2.12)** for an operational condition which is T=0.21m vessel ($1 < Q_g < 15$ Lmin^{-1}, and $6.67 < N < 13.33$rev.s^{-1}). The correlation is:

$$k_La = 0.04\left(\frac{P_g}{V}\right)^{0.47} \tag{2.13}$$

Normally, information about the local k_La is important in the study of gas-liquid stirred tanks to spot the occurrence of very low k_La values, often referred to as 'dead zones'.

Besides of k_La, gas hold-up and bubble sizes are very important parameters within stirred tank that need to look into account. Many correlations have been proposed by many researchers and normally they used Rushton turbine in a standard design of tank (Gimbun et al., 2009). Most of the researchers were correlated the same correlation of gas hold-up (α_g) as below:

$$\alpha_g = C_h \left(\frac{P_g}{V_l}\right)^A v_{sg}^B \tag{2.14}$$

P_g represent the gassed power, V_l is the volume of liquid tank, and v_{sg} is the superficial gas velocity. Moreover, Bakker et al. (1994b) recommend an equation of this form with values for air-water system of C_h = 0.16 + 0.04, A = 0.33 and B = 0.67.

As stated in the previous statement, bubble size is very important to be considered in gas-liquid stirred tank because bubbles are existed while the impeller is rotated. Besides, the bubbles have many sizes and required correlation that fixed with their condition. Bouaifi et al. (2001) have studied on overall gas hold-up, volumetric mass transfer coefficient, liquid side mass transfer coefficient, volumetric interfacial area, bubble size and bubble distribution in bubble columns and gas-liquid STR. From their study, they did found that the bubble is generally in ellipsoids shape. Therefore, they calculated the local bubble diameter using following equation:

$$d_{bi} = (a^2 b)^{1/3} \tag{2.15}$$

Where a and b are the diameter and width of that bubble shape. Despite of that, they were selected 150-200 bubbles to estimate the *Sauter* mean diameter (d_{bs}). Therefore, Bouaifi et al. (2001) proposed the correlation of “average” bubble size as below:

$$d_{bs} = \frac{\sum_i n_i d_i^3}{\sum_i n_i d_i^2} \tag{2.16}$$

Where n_i is the number of bubbles with the diameter, d_i Interfacial area is a function of bubble size and hold-up, hence it is related to the diameter of bubble size (d_{32}).

Calderbank (1958) reported that the viscous forces do not have effect to the dispersion of the gases in liquids under all condition except the condition where the dispersion is caused by the viscous forces rigorously. Therefore, he claimed that the balance is reached between surface tension forces and turbulent fluctuations and thus, proposed the correlation that fixed with his condition by taking into consideration the size of the bubble within the agitated liquid. The equation as below:

$$d_{32} = 4.15\left[\frac{\sigma^{0.6}}{\rho_L^{0.2}\left(P_g/V\right)^{0.4}}\right]\alpha^{1/2} + 9\times10^{-4}\ \text{metre} \tag{2.17}$$

Where d_{32} *Sauter* mean bubble diameter or surface volume is mean, σ is interfacial tension, ρ_L is density of liquid and α is gas void of fraction. Using similar method, Calderbank (1958) also derived an expression for the gas voidage fraction:

$$\alpha = \left(\frac{U_g\alpha}{V_\infty}\right)^{1/2} + 2.16\times10^{-4}\left(\frac{\rho_L{}^{0.2}\left(P_g/V\right)^{0.4}}{\sigma^{0.6}}\right)\left(\frac{U_g}{V_\infty}\right)^{1/2} \tag{2.18}$$

Where V_∞ is the bubble rise velocity (generally about 0.25m/s for aqueous systems)

2.6 Review Experimental and Numerical Method of STR

Many experimental studies and simulation have been conducted regarding to the performance of gas-liquid stirred tank by many researchers. Some of the most significant work are summarised in **Table 2.2.** Previous studies, some of the researchers conducted experimental and numerical method instantaneously for their research (Bakker and Akker, 1994a; Deen et al., 2002; Sun et al., 2006; Murthy et al., 2008; Taghavi et al.,2010), but some of them just conduct either experiment (Bakker and Akker, 1994b; Myers et al., 1994; Laakkonen et al., 2005; Kapic and Heindel, 2006; Bombac and Zun, 2006; Ford et al., 2008; Qingbai and Gance, 2010) or numerical method (Gentric et al., 2005; Khopkar et al., 2005; Luchang et al., 2007; Ranade et al., 2008; Gimbun et al., 2009; Luchang et al., 2010; Ahmed et al., 2010). The good performance of stirred reactor can be achieved by making adjustment on the inappropriate operating hardware and parameters. The parameters like impeller shapes (Murthy et al., 2008; Sun et al., 2006), impeller speed (Ford et al., 2008; Taghavi et al., 2010; Wang et al., 2006; Qingbai et al., 2010; Ahmed et al., 2010), impeller position (Bakker and Akker, 1994), sparger position (Bakker and Akker, 1994), aeration rate (Bakker and Akker, 1994; Wang et al., 2006), have been studied by them experimentally and numerically.

The flow patterns of gas-liquid in STR are complicated to predict and have been studied by many authors by using the CFD (Khopkar and Ranade, 2005; Murthy et al., 2008; Gentric et al., 2005; Deen et al., 2002; Ahmed et al., 2010; Taghavi et al., 2010). Ford et al. (2008) and Heindel et al. (2008) have been used X-ray Computed Tomography to measure the local time-averaged gas hold-up in STR but this equipments is very expensive and cannot measure the different size of gas bubbles that coexist in gas-liquid STR. Nevertheless, other authors also utilized the sophisticated equipments in their experiments to measure the flow pattern in gas-liquid STR like Gamma Ray Tomography, GRT (Veera, 2001; Bukur et al., 1996), Particle Image Velocity, PIV (Deen et al., 2002; Laakonen et al., 2005), Laser Doppler Anemometry, LDA (Rutherford et al., 1996). Alternatively, a computational method like a combination of computational fluid dynamics (CFD) may also be capable to provide a detail description of two-phase flow in aerated stirred tanks at far lower investment and running cost. Therefore, this study is devoted to the development of a computational approach suitable for predicting the two-phase flow in gas-liquid stirred tanks.

METHOD	Experiments					Numerical / Simulation					Remarks
PARAMETERS/ AUTHORS	Buble size	Power no.	Two-phase flow	Hold-up	k_La	Buble size	Power no.	Two-phase flow	Hold-up	k_La	
Ahmed et al. (2010)						yes	yes	yes	yes	no	Carried out multiphase CFD simulation to identify various flow regimes and hydrodynamic parameters in gas–liquid stirred tank bioreactor with dual Rushton turbine impellers
Bakker and van den Akker (1994a)	yes	yes	yes	yes	yes						Lack of local hold-up measurement & numerical result at impeller discharge. One way coupling BDM solved on a result of single phase CFD simulation
Bakker and van den Akker (1994a)						yes	no	yes	yes	yes	Lack of mass transfer measurement, so can be improved by matching the position of extremes in the spatial distribution.
Bombac and Zun (2006)	no	yes	yes	no	no						Gas hold-up not taken into account. Comparison single, dual, triple impeller.
Deen et al. (2002)	no	yes	yes	no	no	yes	yes	yes	no	yes	Distorted drag model gave the best correspondence with experimental result.
Ford et al. (2008)	No	yes	no	yes	no						RDT, gas sparged from a sparger ring Assessment on the gas hold-up in an aerated stirred tank using a x-ray tomography under flooding, loaded and fully dispersed condition

Gentric et al. (2005)						yes	yes	yes	yes	no	Comparison between 2 industrial gas-liquid reactors
Han et al. (2007)						no	no	yes	yes	no	Further study is necessary on the mechanisms of bubble-eddy interaction by means of combining experimental method. It should involve the effect of bubble sizes on the interaction
Han et al. (2010)						yes	no	yes	yes	no	Describe the interaction between turbulent eddy & bubble. Develop EBI in DRW framework.
Kapic and Heindel (2006)	no	yes	no	no	yes						$k_L a$ measured via dissolved oxygen probe but such measurement is a local value at the probe location only
Khopkar et al. (2005b)	no	no	yes	yes	no	yes	yes	yes	yes	no	Combined CARPT & CT measurement on aerated stirred tank hold-up and mean velocity. CFD simulation using a monodispersed bubble size and consequently the mean velocity at impeller discharge is not predicted correctly. The gas hold-up is not predicted correctly
Murthy et al. (2008)	no	no	yes	yes	no	yes	no	yes	no	no	Discrepancy in prediction of induction rate can be improved by employ more reliable inter-phase momentum exchange.
Ranade et al. (2008)						yes	yes	yes	yes	no	$k_L a$ is not considered in in momentum balance equations.

Scargiali et al. (2007)						yes	yes	yes	yes	no	To get better result : develop bubble breakage & coalescence
Sun et al. (2006)	no	no	yes	yes	no	yes	no	yes	yes	no	Gas bubble size is major factor to be incorporated into numerical program for further improving accuracy of simulation.
Taghavi et al. (2010)	no	yes	yes	no	no	no	yes	yes	no	no	Calculate power using torque equation
Wang et al. (2006)	no	no	no	yes	no	no	no	yes	yes	no	Using fibre optic technique to show different gas-liquid flow patterns including flooding
Xiao et al. (2007)	no	yes	no	no	yes						k_La versus energy dissipation rate in horizontal tank better than vertical tank
Zhang (2000)						yes	no	yes	yes	no	Injection bubble generate a well mixing flow.

Table 2.2: Summary of experimental and numerical method studies of flow pattern in gas-liquid stirred tank

2.7 Summary

The applications of gas-liquid stirred tank have been outlined in this chapter. From the description above, shows that stirred tank is widely used especially in bio-fermentation process and chemical process. Besides that, the criterions of flow regime have been discussed from flooding, loading to fully dispersion. Flooding is undesirable because it lead to the low performance of gas-liquid stirred tank. Moreover, the empirical equations that involved throughout this study have been described briefly. On the other hand, a summary on the previous study that related with this study via experiment and numerical simulation were summarized.

CHAPTER 3

METHODOLOGY

3.0 COMPUTATIONAL APPROACH

3.1 Overview

This chapter mainly described the modelling strategy and set up of gas-liquid stirred tank and also the computational approach applied for gas-liquid stirred tank modelling of multiphase flow including the turbulence model, Eulerian-Eulerian model, Multiphase Reference Frames (MRF) and drag model. The mathematical model used to account for turbulence flow of multiphase system is also described. In the multiphase model, Eulerian-Eulerian model is used. Besides that, in turbulence model, two-phase standard k-ε is employed. Turbulence model and multiphase model have been run in standard FLUENT model. Other than that, drag model for bubble is employed due to the presence of different sizes of bubbles in gas-liquid stirred. In order to conduct CFD in this current work, a few steps are required to analyze the performance of gas-liquid stirred tank at different flow regime from loading to gas dispersion. The overall research methodology consists of two main steps. First step is about drawing the gas-liquid stirred tank geometric and set the set-up and for the second step is about analysis the flow in gas-liquid stirred tank as in **Figure 3.1** below:

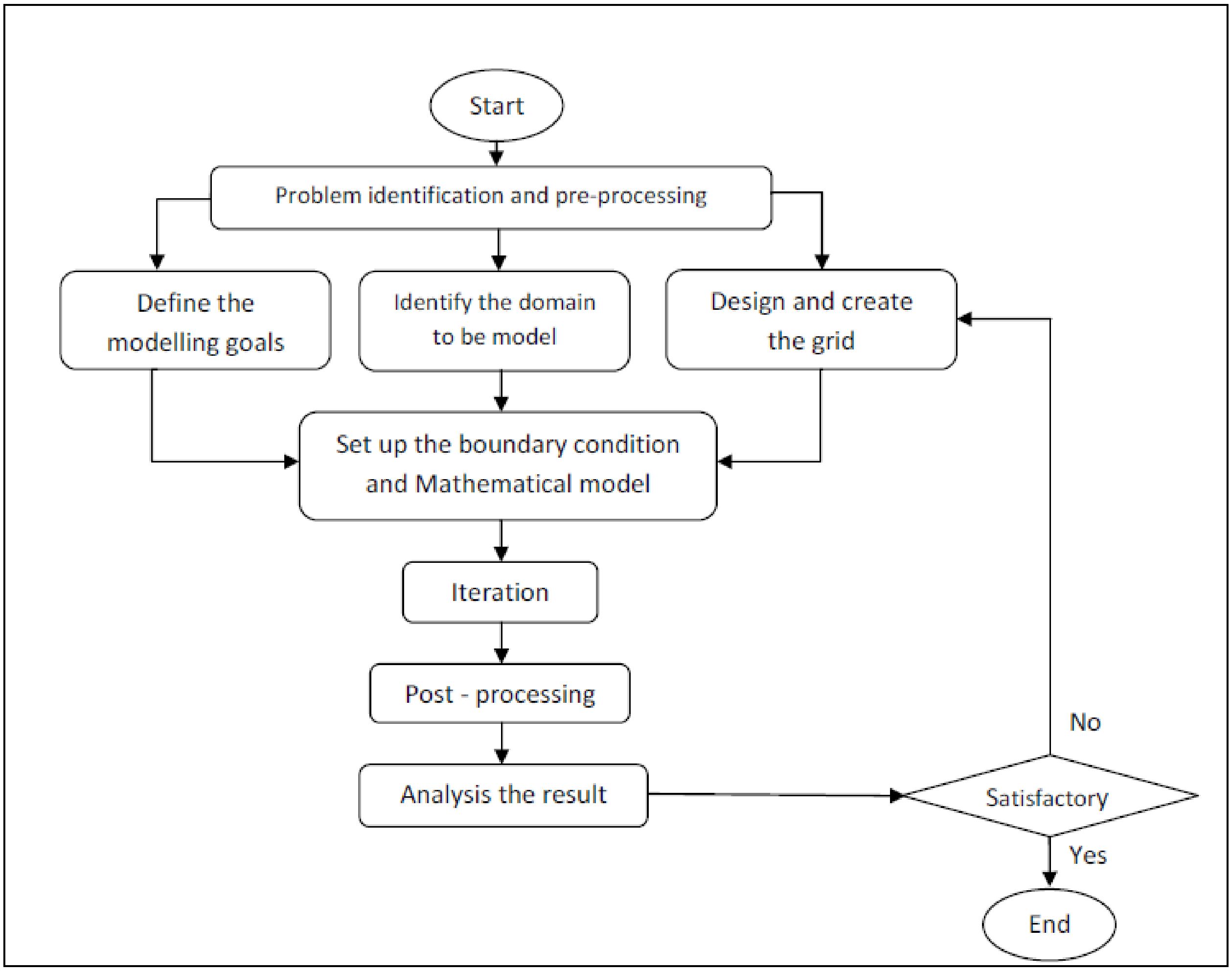

Figure 3.1: Steps on CFD analysis

3.2 Gas-Liquid STR Dimension

The modelling result presented in this chapter is mainly taken from Ford et al. (2008). The stirred tank configuration and dimension of the tank is based on the experimental studied by Ford et al. (2008). The dimension is illustrated in **Figure 3.2.** The system is a dished-bottomed tank made from acrylic with an internal diameter of T=0.21 m. The tank has four equally spaced baffles of width 0.0018 m and thickness of 0.006 m. The height of the tank is same as the internal diameter, H = T = 0.21 m. Type of impeller used for this study is Rushton-type impeller which is having 6 blades with diameter, D = 0.076 m. the impeller blade have a height of 0.019 m and thickness of 0.003m and was located at

0.057 m from the bottom of stirred tank which correspond to a clearance C=0.27T with a hub having diameter 0.031m. This tank was modelled with a ring sparger having diameter 0.051m. For this study, the power drop and gas hold-up were measured at constant gas flow rate; 9 LPM but different impeller speed (N); 200 rpm, 350 rpm, 525 rpm and 700 rpm.

3.3 Modelling Strategy

In this study, Gambit 2.2 was employed to create a structured, non-uniform multi block grid with the impeller (rotating) and static zones being separated by an interface to enable the use of Multiple Reference Frames (MRF) technique. The computational grid for RANS modelling was defined by 393830 of structured, non-uniform distributed hexahedral cells representing only half tank domain for a smaller tank with the volume of the tank is 7.1L. (**Figure 3.2**) a local grid refinement containing 12716 cells was applied in the rotating zones to better resolve this highly turbulent region. All simulations were performed using a half tank grid made of 100% hexahedral elements which is desired for a better prediction accuracy and minimum numerical diffusion. According to Derksen et al. (1999) a proper grid for stirred tanks modelling should be able to resolve the trailing vortex behind the impeller blade. They recommended using at least 8 nodes along the impeller height to resolve the trailing vortex for RANS modelling. The trailing vortex is an important flow feature in stirred tanks which significantly affects prediction of the turbulence and mean flow. In this study, 10 nodes along the impeller blade height were assigned for the RANS modelling. The interphase drag coefficient was estimated using the standard Schiller-Naumann drag model (Schiller and Naumann, 1935). The impeller movement was modelled using the multiple reference frame (MRF) technique and the Eulerian-Eulerian approach was employed for the multiphase modelling. The turbulence was modelled using the two-phase standard k-ε model. The diameters of the bubble size have been determined by employed the equation proposed by Calderbank (1958) (**Eq. 2.17**) for the *Sauter* mean bubble size.

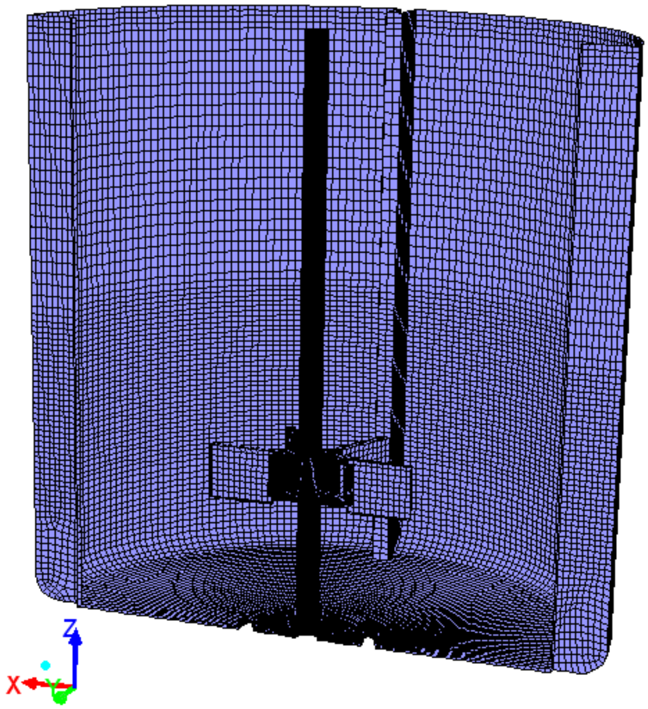

Figure 3.2: Surface mesh of half stirred tank

3.4 Two Phases Flow Modelling

In this current study, the Eulerian-Eulerian model will be employed for gas-liquid stirred tank for multiphase flow throughout simulation. This model is used to model droplets or bubbles of secondary phases dispersed in continuous fluid phase (primary phase). Besides that, this model is allows for mixing and separation phases. From this model, turbulence model can be solved for each phase and besides, the momentum, enthalpy and continuity equations for each phase and tracks volume fractions. Moreover, this model uses inter-phase drag coefficient and allows for virtual mass effect and lift forces. A general multiphase system consists of interacting phases dispersed randomly in space and time for example Ishii (1975) used the averaging technique and closure assumptions to model the unknown quantities. The volume fractions sum to unity and are governed by the following continuity equations:

$$\frac{\partial}{\partial t}\left(\alpha_l \rho_l\right) + \nabla.\left(\alpha_l \rho_l \, \vec{u}_l\right) = 0 \tag{3.1}$$

Where α_l is the liquid volume fraction, ρ_l is the density, and $\vec{u}_l$ is the velocity of the liquid phase. **Eq. (3.1)** is equal to zero because the mass transferred between phases is negligibly small and thus it is not included in the right hand-side of equation (**3.1**). For the volume fraction of the gas phase, a similar equation is solved by replacing the subscript l with g. The momentum balance for the liquid phase is:

$$\frac{\partial}{\partial t}\left(\alpha_l \rho_l \, \vec{u}_l\right) + \nabla.\left(\alpha_l \rho_l \, \vec{u}_l \, \vec{u}_l\right) = -\alpha_l \nabla P + \nabla.\,\bar{\bar{\tau}}_l + \vec{F}_{lg} + \alpha_l \rho_l \vec{g} + \vec{F}_{lift,l} + \vec{F}_{vm,l} \tag{3.2}$$

Where $\bar{\bar{\tau}}_l$ is the liquid phase stress-strain tensor, $\vec{F}_{lift,l}$ is a lift force, $\vec{g}$ is the acceleration due to gravity and $\vec{F}_{vm,l}$ is the virtual mass force and a similar equation is solved for the gas phase. $\vec{F}_{lg}$ is the interaction force per unit volume of mixture between phases due to drag.

The more significant of force for larger bubble is lift forces due to the velocity gradients in liquid phase. The lift force acting on a gas phase in liquid phase can be estimated from:

$$\vec{F}_{lift,g} = -C_L \rho_l \alpha_g \left(\vec{u}_l - \vec{u}_g\right) \times \left(\nabla \times \vec{u}_l\right) \tag{3.3}$$

Where C_L is a lift coefficient has a value 0.5. A similar lift force is added to the right-hand side of the momentum equation for both phases $\left(\vec{F}_{lift,g} = -\vec{F}_{lift,l}\right)$.

As pointed out by Scargiali et al. (2007) the effects of the virtual mass and lift forces are almost negligible, despite a significant increase in computational expenses and convergence difficulties. However, the effect of the drag force is largely predominates in gas-liquid stirred tank compared to other inter-phase force. Drag model employed in this current work will be discussed in Section 3.5.

3.5 Drag Force Modelling

The inter-phase force term $F_{\beta\alpha}$ represents the interaction forces between the continuous and the dispersed phase. This force consists of four terms which are Basset history force, lift force, virtual mass force and the interface drag force (Ranade, 1992). These terms are being introduced due to a few reasons for such as if the slip velocity is constant, the force is known as 'drag' while the rest of terms mentioned before are being introduced due to non-uniform motion. This can be concluding as below:

$$F_{\beta\alpha} = F_{lg}(F_{VM}+F_{lift} + F_{basset}+F_{wall\ lubrication\ldots}) \tag{3.4}$$

From previous studies, it is often found that when compared to the drag force, the other inter-phase forces are negligible (Lane et al., 2002). However, bubbles experiences lift force due to the vorticity and shear in the continuous phase flow field. Hence, lift force is significant if the velocity gradients are large due to the directly proportional of lift force to the vector product of the slip velocity and the curl of liquid velocity. Besides that, Basset force cannot be considered because it is time-consuming when it comes to evaluate because it is involved history integral and its magnitude is much smaller than inter-phase drag force. While Khopkar et al. (2003) reported on their numerical experiments, the effect of the virtual mass is not significant in the bulk region of stirred vessel. Therefore, in order to reduce the computational costs, drag force is the only inter-phase force that will be considered in this current study as the inter-phase momentum exchange term by neglecting the effects of lift force, virtual force and Basset force. Thus, the $\vec{F}_{lg}$ is represented by a simple interaction term for the drag force, given by:

$$\vec{F}_{lg} = -\frac{3\alpha_g\alpha_l C_D|\vec{u}_g - \vec{u}_l|(\vec{u}_g - \vec{u}_l)}{4d_b} \tag{3.5}$$

Where C_D is a drag coefficient and d_b is the *Sauter* mean bubble diameter. The drag model employed has a significant effect on the flow field of the aerated flow, as it is related directly to the bubble terminal rise velocity.

Normally, the standard FLUENT drag model is only suitable for solid spheres. The equation given as below:

$$C_D = f\left(\frac{\rho_l|\vec{u}_g-\vec{u}_l|d_{32}}{\mu_l}\right) \tag{3.6}$$

Where d_{32} is referring to the bubble size. However, to conduct this current study, the drag model above cannot be relies on as overall of the bubble that present inside the gas-liquid stirred tank. This is because bubbles do not have one shape. Therefore, this study was developed the drag model changes due to the different shape of the bubble that may present in the gas-liquid stirred tank. Thus, the drag model of Schiller and Naumann (1935) will be used. The equation given as below:

$$C_D = \frac{24}{Re_b}(1 + 0.15{Re_b}^{0.687}) \tag{3.7}$$

where the bubble Reynolds number, Re_b is defined as:

$$Re_b = \frac{\rho_l|\vec{u}_g-\vec{u}_l|d_b}{\mu_l} \tag{3.8}$$

The Schiller and Naumann (1935) drag model is best suited for a spherical bubble, i.e. in air-water for a bubble with a diameter smaller than 3 mm. In this study, equation of Calderbank (1958) (**Eq 2.17**) has been applied to determine the diameter of bubble size at different impeller speed based on the gas voidage fraction given by Ford et al. (2008).

3.6 Turbulence Modelling

In FLUENT, there are three different options available for turbulence modelling of multiphase flow which are mixture k-ε, dispersed k-ε and two-phase k-ε models (FLUENT 6.3, 2006). All these three models have different equations to account for turbulence viscosity even used the same model constants. But for this study, dispersed k-ε model has been utilized to solve the standard k-ε equations.

Dispersed k-ε model is suitable when the first phase is clearly continuous while second phase is dilute. Hence, the dispersed k-ε turbulence model is used to solve the standard k-ε equation for the primary phase and used Tchen's theory of dispersion for second phase. The turbulent viscosity is based on the *k*-*ε* model and formulated as follows:

$$\mu_{t,l} = \rho_l C_l \frac{k_l^2}{\varepsilon_l} \tag{3.9}$$

The turbulent kinetic energy, *k* and energy dissipation, *ε* are calculated from their transport equations in the dispersed k-ε model given by:

$$\frac{\partial}{\partial_t}(\rho_l \alpha_l k_l) + \nabla.(\rho_l \alpha_l \vec{u}_l k_l) = \nabla.\left(\alpha_l \frac{\mu_{t,l}}{\sigma_k} \nabla \mathrm{k}_l\right) + \alpha_l G_{k,l} - \alpha_l \rho_l \varepsilon_l + \alpha_l \rho_l \Pi_{k,l} \tag{3.10}$$

$$\frac{\partial}{\partial_t}(\rho_l \alpha_l \varepsilon_l) + \nabla.(\rho_l \alpha_l \vec{u}_l \varepsilon_l) = \nabla.\left(\alpha_l \frac{\mu_{t,l}}{\sigma_\varepsilon} \nabla \varepsilon_l\right) + \alpha_l \frac{\varepsilon_l}{k_l}\left(C_{1,\varepsilon} G_{k,l} - C_{2,\varepsilon} \rho_l \varepsilon_l\right) + \alpha_l \rho_l \Pi_{\varepsilon,l} \tag{3.11}$$

$G_{k,l}$ is the rate of production of turbulent kinetic energy and it has a similar form to the one applied for single phase flow and described as:

$$G = \tau_L : \nabla u_L \tag{3.12}$$

The terms $\Pi_{k,l}$ and $\Pi_{\varepsilon,l}$ represent the influence of the dispersed phase on continuous phase. For turbulent dispersed two phase flow, the exchange term in the turbulent kinetic energy can be derived from the equation for the individual fluctuations as given below:

$$\Pi_k = \alpha_k \rho_k \frac{f_{drag}}{\tau_{ki}} (k_{ik} - 2k_k) \qquad (3.13)$$

The contribution to the equation is modelled according to Elgobashi and Abou-Arab (1983):

$$\Pi_\varepsilon = C_{\varepsilon 3} \frac{\varepsilon_k}{k_k} \Pi_k \qquad (3.14)$$

The turbulent quantities for the dispersed phase like turbulent kinetic energy and turbulent viscosity of the gas are modelled following Mudde and Simonin (1999) using the primary phase turbulent quantities (FLUENT 6.3, 2006). The model constants for dispersed k-ε model are similar to those of mixture k-ε model and two-phase k-ε model as tabulated in **Table 3.1** below:

C_μ	$C_{\varepsilon 1}$	$C_{\varepsilon 2}$	$C_{\varepsilon 3}$	σ_k	σ_ε
0.09	1.44	1.92	1.3	1	1.3

Table 3.1: Constant of dispersed k-ε model

3.7 Impeller Modelling

A few papers in the literature deal with CFD simulation of gas–liquid mixing tanks. These studies consider simple agitating devices for which experimental data are available, i.e., often, one Rushton turbine in its standard configuration. Most of the time, Eulerian simulations are carried out with the k-ε turbulence model. Modelling the impeller is not an easy thing to be carried out. This part is very crucial and we need to choose method that suitable to be employed. The main difficulty lies in modelling is the motion of the rotating impeller past the stationary tank walls and baffles.

There are many different of methods in order to conduct the impeller's modelling; time averaged methods (2-D or 3-D), snapshot methods (3-D) and transient methods (3-D). The objective for time-averaged method is to calculate time averaged flow field in the vessel. Besides, this method is not consider the details of flow around impeller blades. The impeller will be replaced with a simple, disk style region hence, easy to mesh with fewer cells than other methods. Furthermore, this method is fast flow field calculations and fast species mixing and particle tracking calculations. Nevertheless, this method also has its own weaknesses. It is very complex to use for multiphase flow (e.g: gas-liquid flows). Besides that, the velocity data is needed for the particular impeller at the particular Reynolds number whereby this data can be obtained from experiment or other CFD simulation.

Snapshot method also known as steady-state method or rotating coordinate system which is this method is only to calculate one flow field for one given impeller position. This method is not required experimental data. In FLUENT, this is done by having a separate fluid region that contains the impeller. Hence, for this region, a Multiple Reference Frame with a rotational motion is specified. The advantage of this method is that no empirical information is needed to set the boundary conditions. The inner part of the stirred tank will be described as the coordinate system that co-rotates with the impeller while the outer part of the stirred tank will be described in a fixed coordinate frame.

Moreover, inner-outer method (IO) also has the same concept like MRF method. The former was introduced by Luo et al. (1994). Nevertheless, they have one distinct difference among MRF and IO method. In IO, the calculation domains of the two parts have a small overlap unlike MRF. Besides that, in order to ensure the continuity across the interface between two parts, a number of outer iterations are required (Deen et al., 2002). This is shown that IO method is required extra time for calculation compared to MRF.

Other than that, sliding grid method (SG) also used rotating coordinate system. Perng and Murthy (1992) is the first group applied this method. This method can be categorized as transient method as mentioned above. This is because both coordinate system and the grid of the inner part are rotating thus making them computationally more expensive than MRF method (Deen at al., 2002). The difference between SG, MRF and IO method is no extra iterations are necessary to conduct because the entire domain can be solved as a whole. According to Tabor et al. (1996), MRF method is better than SG method on their research about observing the vortices trailing from impeller blades.

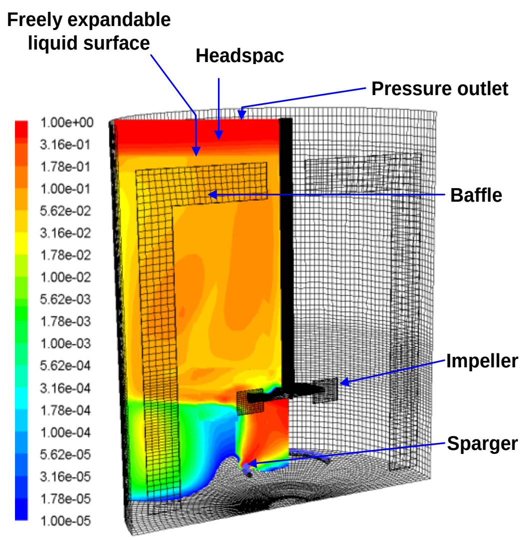

Figure 3.3: Boundary condition of gas-liquid STR simulation.

MRF method can be used when experimental impeller data is not available and the impeller geometry is known. Therefore, in this study, a Multiple Reference Frame (MRF) model has been applied to represent the impeller rotation for all the RANS simulation as we know the main issues when simulating stirred tank is that the problem geometry varies with time due to the relative motion between the impeller and the baffles.

3.8 Computational Fluid Dynamics (CFD) of STR

Gas-liquid stirred tank normally used in bio-chemical fermentations and chemical process. Many studies have been carried out by researchers in order to investigate the performance of gas-liquid stirred tanks experimentally (Bakker and Akker, 1994b; Myers et al., 1994; Laakkonen et al., 2005; Kapic and Heindel, 2006; Bombac and Zun, 2006; Ford et al., 2008; Qingbai and Gance, 2010) or via numerical simulation (Gentric et al., 2005; Khopkar et al., 2005; Luchang et al., 2007; Ranade et al., 2008; Gimbun et al., 2009; Luchang et al., 2010; Ahmed et al., 2010). A detailed review of the measurement techniques employed for gas-liquid stirred tank is outlined previously in Chapter 2. However, a comprehensive method like the combination of CFD, population balance model, PBM (bubble coalesce and bubble breakage) and drag model changes by Ishii and Zuber (1979) and Schiller and Naumann (1935) still has not been yet published.

3.9 Summary

RANS simulation has been used to conduct this study. Method used to conduct this study are consists of turbulence model of standard k-ε model and multiphase model by employed the Eulerian-Eulerian approach within the standard FLUENT models. Besides that, the drag model chose to be employed in this study was Schiller & Naumann (1935) for the bubble size. While Calderbank (1985) equation has been utilized to determine the *Sauter* mean bubble diameter at different impeller speed based on the gas void fraction from the previous study by Ford et al. (2008).

CHAPTER 4

RESULTS & DISCUSSIONS

4.1 Introduction

In this chapter, the result will be discussed based on the objective (Chapter 1) and using the methods that have been mentioned in Chapter 3. This study was conducted CFD simulation instead of using experimental set up due to the higher cost investment and to reduce the time taken to evaluate the performance of gas-liquid stirred tank if using experimental set up. Two scope of study have been decided in the early of this research which are to study the power drop and gas hold-up in gas-liquid stirred tank at various flow regime (flooding, loading, fully gas dispersed). The result were obtained from the CFD simulation for different regime; flooding, loaded, and fully dispersion by employed the method in Chapter 3 with different of impeller speed, will be compared with the result obtained by Ford et al. (2008).

4.2 Prediction of Gas-Liquid Hydrodynamics

First, the CFD simulation were validated against experimental data using two-phase X-ray computed tomography measurements reported by Ford et al. (2008) for a stirred tank with constant bubble size. Details of the geometry and operating parameters of Ford's tank are given in **Table 4.1**. The initial simulation using constant bubble size is required before performed other simulation with different bubble size for different impeller speed by using the data of Ford et al. (2008) on the global gas hold-up (void fraction). Therefore, a realistic initial bubble size of 3.5 mm was employed throughout the tank for the initial simulation. For this validation step, it has to be noted that this initial bubble size does not really matter in the end of CFD-SN simulation, as the final bubble size will be determined by using model proposed by Calderbank (1958) for the *Sauter* mean bubble size. The bubbles were assumed to be spherical and the Schiller and Naumann (1935) drag model was employed to estimate the drag coefficient. The CFD results were time-averaged over all blade angles and compared with Ford et al. (2008) X-ray computed tomography (X-ray CT) measurements.

A simulation using the non-uniform bubble size was next performed to evaluate the power consumption and gas hold-up at different regime from flooding to complete dispersed transition regime. In this study, the bubble shape was assumed to be spherical rigid bubbles throughout the tank during the simulation. The interphase drag coefficient was estimated using the standard Schiller-Naumann drag model (Schiller and Naumann, 1935) as well as this model is suitable for spherical rigid bubbles. Predictions of the CFD-SN model were slightly better than the one with a constant bubble size. Although there is not much improvement when the CFD alone and spherical drag model (CFD- SN) are employed. Lane et al. (2002) has pointed out that Brucato et al.'s drag model led to a wrong prediction of gas hold-up distribution; higher gas hold-up near the bottom of the tank. Nevertheless, Ford et al.'s result regarding on the gas hold-up by taking the consideration the distance from the bottom of impeller at z-axis and hold-up along x-axis at height z=0.8cm has the good agreement with Lane et al. (2002); higher local gas hold-up near the impeller with the increasing of impeller speed. The impeller movement was modelled using the multiple reference frame technique and the Eulerian-Eulerian approach was employed for the multiphase modelling. The turbulence was modelled using the two-phase standard k-ε model.

PARAMETER	Ford et al. (2008) Case 1	Ford et al. (2008) Case 2	Ford et al. (2008) Case 3	Ford et al. (2008) Case 4
T=H (m)	0.21	0.21	0.21	0.21
Tank type	Dished bottom tank	Dished bottom tank	Dished bottom tank	Dished bottom tank
Impeller type	Rushton turbine	Rushton turbine	Rushton turbine	Rushton turbine
Impeller diameter(m)	0.076	0.076	0.076	0.076
Sparger type	Ring	Ring	Ring	Ring
Sparger diameter(m)	0.051	0.051	0.051	0.051
Q_g (m^3/s)	0.00015	0.00015	0.00015	0.00015
N (rpm)	200	350	525	700
Void of fraction	0.029	0.033	0.045	0.06
F_{lg}	0.1025	0.0586	0.039	0.029
Fr	0.086	0.2637	0.59	1.055
Re	19253.33	33693.33	50540	67386.67
Volume(m^3)	0.0073	0.0073	0.0073	0.0073
d_{32} (Calderbank, 1958)	0.009	0.0056	0.005223	0.0039

Table 4.1: Geometry for stirred tank at different impeller speed.

4.3 Prediction of Aerated Power Number

In chapter 2, the prediction of the gassed power input have been explained where P_g can be estimated from the moment acting on the shaft and impeller or baffles and tank wall which known as torque, (Γ) (refer **Eq. 2.11**). In this work P_g was calculated using the moment acting on the impeller and shaft, because to produce a more reliable prediction than the moment acting on baffle and wall. Many correlations are available for calculating the gassed and ungassed power number of stirred tanks agitated by a Rushton turbine. Ford et al. (2008) performed extensive experiments in two phase within aerated stirred tanks fitted with a Rushton type impeller, they reported that Pg/Po drop little by little when the impeller speed is increased from 200 rpm to 700 rpm but the P_g and P_o alone increased drastically when the impeller speed is increase. According to Nienow (1998), the ungassed power number for STRs with Rushton-type impeller is to be 5. Ford et al. (2008) were reported that the average ungassed power number used in their study is 4.8. In this study, the average ungassed power number used is 5.

For this study, the gas power numbers have been measured based on the moment acting on the impeller and shaft at constant aeration rate (Q_g) 0.00015 m^3/s. **Table 4.2** shows the gas power numbers obtained for different impeller speed for different regime transition via CFD simulation.

Impeller speed	**Q_g**	**Torque, Γ(CFD)**	**F_{lg}(CFD)**	**F_{lg} (Ford et al.(2008))**	**N_{pg}(CFD)**	**N_{pg} (Ford et al.(2008))**
200	0.00015	0.014268	0.1025113	0.105	3.182	3.6
350	0.00015	0.040664	0.05857789	0.06	2.961	3
525	0.00015	0.096315	0.03905192	0.042	3.117	2.4
700	0.00015	0.47913	0.02928894	0.03	8.723	2.45

Table 4.2: Gassed power number and flow number at different impeller speed.

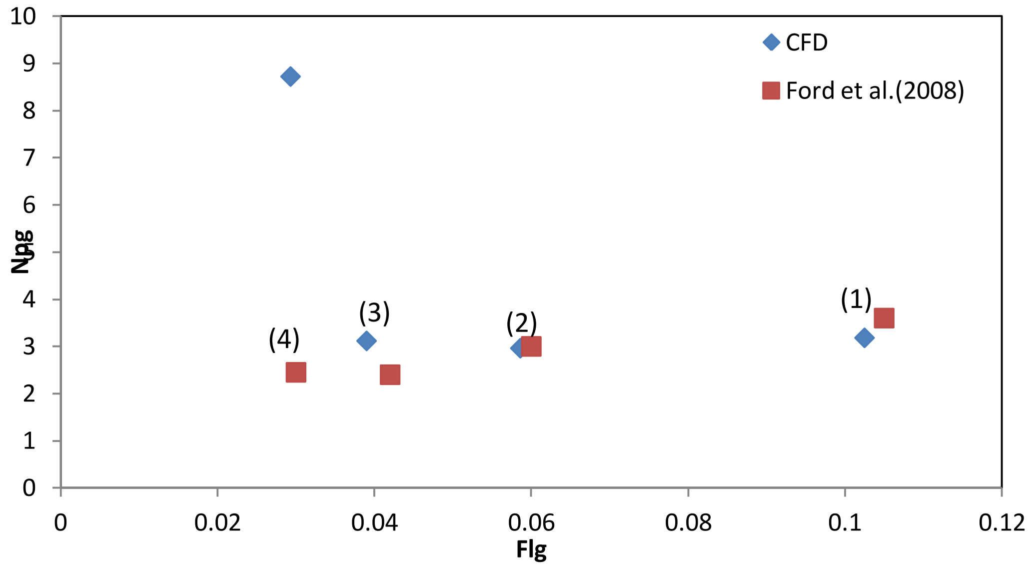

Figure 4.1: Graph of gassed power number vs. flow number at constant flow rate

The graph plotted at **Figure 4.1** is based on the data provided at **Table 4.2** by comparing the gassed power number and flow number obtained via CFD for this study with the result obtained by Ford et al. (2008) at constant air flow rate, Q_g which is 0.0015 m^3/s. The locations of the data described in this study are identified by the solid symbols corresponds to: (1) 200 rpm; (2) 350 rpm; (3) 525 rpm; (4) 700 rpm. From **Figure 4.1**, the gassed power number obtained from this study is not much different with the gassed power number obtained by Ford et al. (2008) and having good agreement with the Ford's data. Nevertheless, there is a discrepancy between the predicted relative power number from CFD simulation and Ford et al.' s result at impeller speed 700 rpm, location noted as (4). This is because of the moment that acting on the impeller and the shaft is high that corresponds to the higher of gas power number as well as the equation provided (**Eq 2.1**).

From the **Figure 4.1**, the impeller speed is decrease from left to the right (200 rpm-700 rpm). At low impeller speed which is 200rpm (1) and constant air flow rate (Q_g) which is 0.00015 m^3/s, flooding will be occurred due to high gas flow number (F_{lg}) and high gas power number (N_{pg}). This is due to the bubbles not being affected by the low impeller speed when the bubbles rise vertically upward to the headspace of the stirred tank. Thus, it leads to the flooding and low mass transfer rate. Another reason of occurring flooding is because of the lack of dispersion throughout the tank. According to Taghavi et al. (2010), at impeller rotational low speed, the power consumption will be low, thus leads to increase the formation of cavity behind impeller blade. At this point, the power drop is increase due to more gas cavities attach to the impeller blade as well as gas is more attracted to the low pressure regions behind impeller blade.

At location noted as (2) the tank is said to be loaded and the impeller acts to disperse the bubbles radially outward in the headspace of the stirred tank. It can be identified when the impeller speed is higher than impeller speed of flooded as well as lower than impeller speed of completely dispersed ($N_f < N < N_{cd}$). According to Ford et al. (2008), loaded regime is still poor gas distribution due to the buoyant forces of the gas being larger than the radial drag force resulting from the liquids mixing even the impeller at this regime is better able to radially distribute the gas. Besides that, across the transitions of flooded to loaded, the bubbles have decreased in size and are located throughout a larger region of the stirred tank. In fact there a very few bubbles below the impeller as well as defined as the characteristics of loaded.

As the impeller speed is increased (4), the transition to complete dispersion occurs through the tank including the below of the impeller. Fully dispersed regime or completely dispersed regime is highly desirable operating regime due to the gas being completely dispersed in at lower power input. According to Ford et al. (2008), bubbles have further decreased in size and they are located throughout the stirred tank. If the impeller speed is increased still further, gas recirculation can be observed (Paglianti et al., 2000). At this point, the gas hold-up is higher, same goes on the mass transfer rate as it is desirable impeller operating speed. However, the result obtained from this study has big divergence with the Ford et al.'s result. The N_{pg} via CFD simulation at 700 rpm is 8.72 while Ford et al.'s N_{pg} is 2.45. This disparity is due to the total moments acting at impeller and shaft is higher for this CFD thus it leads to the higher amount of gas power number. The prediction of gas hold-up will be further discussed in **section 4.3.**

4.4 Prediction of Gas Hold-up

4.4.1 Local gas hold-up

Gas hold-up is prior when it comes to design, scale up and estimate the performance in stirred liquid tank and becomes one of the most important hydrodynamics parameter. Determination of gas hold-up is rely on gas and liquid properties, superficial gas velocity, presence of solids, design of impeller and sparger, internal reactor and power consumption (Ford et al., 2008). Local gas hold-up (ε_g) is highly desirable to be determined and better understanding on how it changes is important to design better stirred tanks. Therefore, this study is conducted the gas hold-up along x-axis at height z = 0.8 cm from bottom of tank and average z-slice hold up at constant air flow rate (Q_g = 0.00015 m^3/s) at different impeller speed; 200 rpm, 350 rpm, 525 rpm and 700 rpm. The CFD simulations were conducted within half tank domain and to be assumed that the same gas-liquid hydrodynamics at another half tank in terms of gas hold-up.

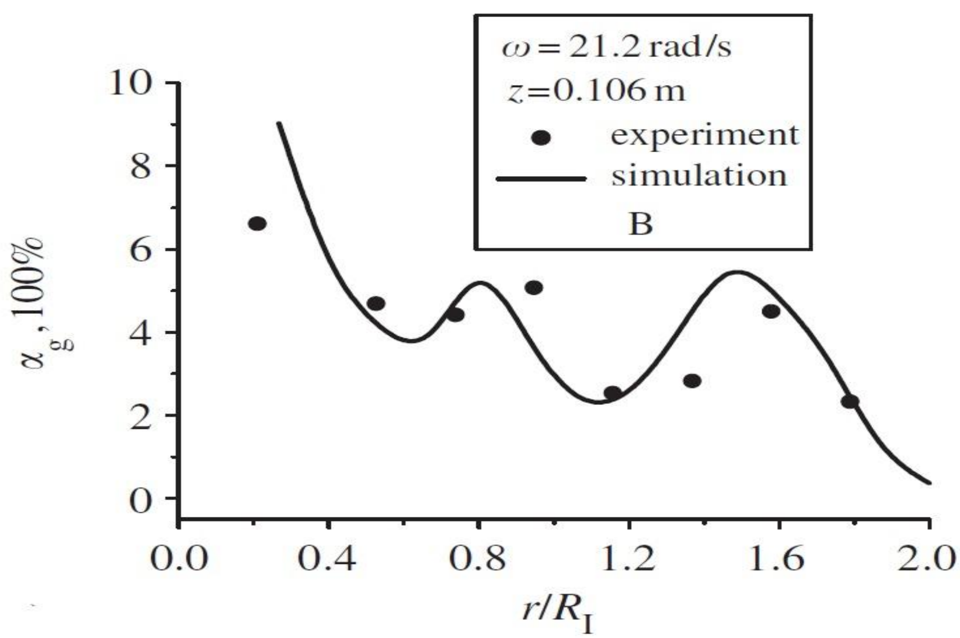

Figure 4.2: Comparison between the simulation and experiment for gas hold up at ω = 21.2 rad/s. (Adapted data from Sun et al., 2006)

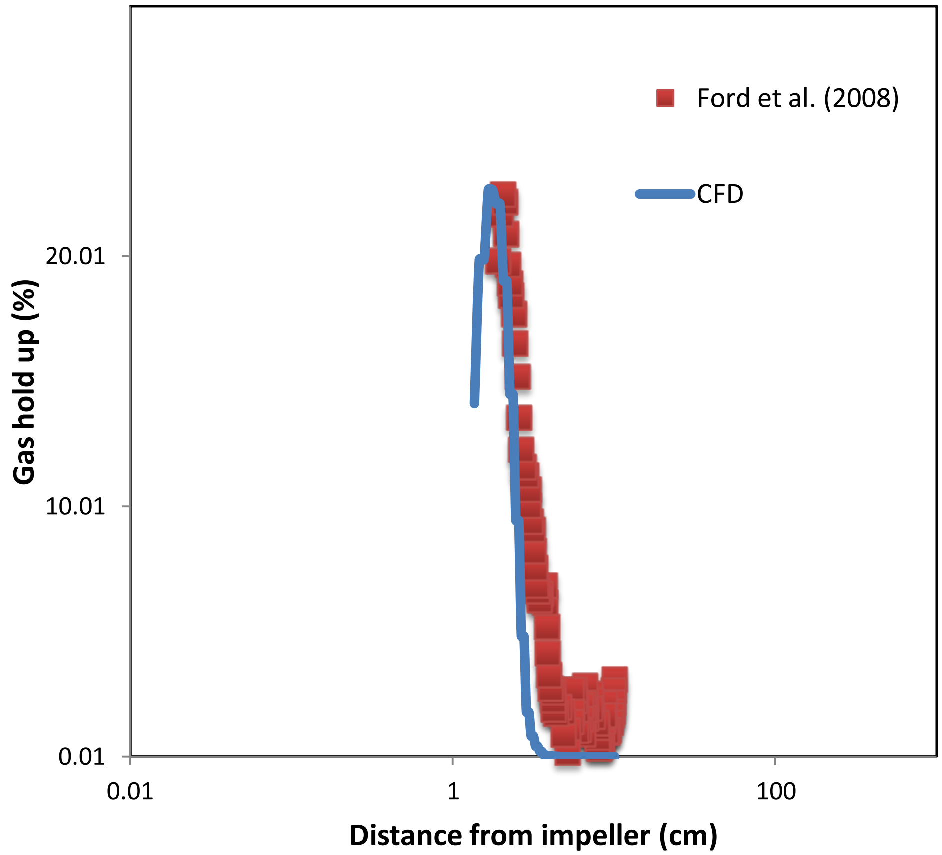

Figure 4.3: Local gas hold-up values along x-axis at height z = 0.8 cm for 200 rpm

Figure 4.3 shows the gas hold-up at impeller speed 200 rpm and constant gas flow rate 0.00015 m^3/s. This result obtained at height, z = 0.8 cm from bottom of tank along the x-axis plane. The data obtained have been compared with the data study by Ford et al. (2008) which observed the gas hold-up by using X-ray computed tomography (X-ray CT). All the graphs plotted at different impeller represent the gas hold-up for half tank domain as well as the other half tank to be assumed has the same gas hold-up. Among all the CFD results at different speed of impeller (**Figure 4.3, Figure 4.4 and Figure 4.5**), in comparison with the result by Sun et al. (2006) shown at **Figure 4.2** at which the impeller speed was conducted at 127.2 rpm having shown an ‘improvement’ on the CFD results to the experimental results by Ford et al. (2008). They were conducted both experimental and simulation study to predict the gas hold up at surface aerated stirred tank at different impeller speed. However, the results show the simulation and experimental method were not predicted well. They reported that their results provide reasonable prediction of gas hold-up at the free surface in comparison with the experimental measurements, but the numerical comparison deep in the bulk liquid phase becomes gradually poor. They have claimed this is due to the negligence of bubble size distribution by used fixed bubble size 3mm. In comparison with the Ford et al.'s data of local gas hold-up, the data obtained from this study via CFD-SN is reasonably accurate with Ford et al.'s data. Even there is a bit diverge, the pattern of the plotted graph is quite similar with Ford et al.'s. From **Figure 4.1**, it has been determined that at impeller speed 200 rpm, the flooding occurred. Therefore, very little gas is located outside the impeller region. This can be shown with the percent of local gas hold-up between **Figure 4.3, Figure 4.4 and Figure 4.5.** at different impeller speed, whereby the smallest percentage of gas hold-up is at **Figure 4.4** which corresponds to smallest impeller speed; 200 rpm with the range below than 25% of local gas hold-up. As the bubble spread out axially far away from the impeller at x-slice, the bubble rise velocity is low due to the low pressure acting on the bubble, therefore the gas hold-up is low and this region is defined as flooded by Warmoeskerken & Smith (1985). At **Figure 4.3**, from this study, the gas hold-up is increasing and decrease back and at after the distance x = 3.46 cm from the impeller, the gas hold-up become constant as there is no gas present. So, from the graph, a good agreement was achieved with prediction by Warmoeskerken & Smith (1985) as the gas hold-up is low when the distance from the impeller increases due to the low pressure acting on the bubbles. According to Ford et al. (2008), the factor tend to lower bubble rise is an increasing in drag as the bubbles spread out.

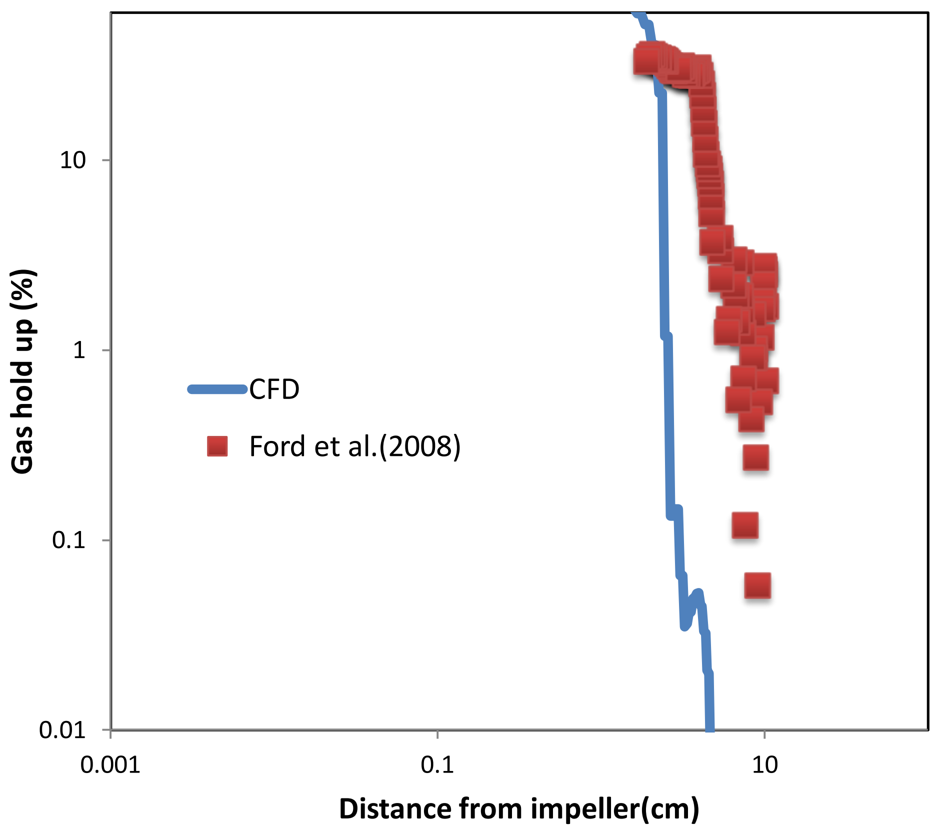

Figure 4.4: Local gas hold-up values along x-axis at height z = 0.8cm for 350 rpm

Figure 4.4 shows the percent local gas hold-up at impeller speed 350 rpm. From this graph, the result obtained via CFD simulation has discrepancy with the data obtained by Ford et al. (2008). First, the local gas hold-up for this study nearest to the impeller is high up to 60% while Ford et al.'s data has the value 33% of gas hold-up at point near to the impeller. Second, the graph pattern is not fluctuate as the Ford et al.'s. The gas hold-up is decreasing as it pass along the x-axis plane at height, z = 0.8 cm and become constant with no present of gas started at point x = 3.26 cm from impeller. According to Ford et al. (2008), at impeller rotation 350 rpm, the gas is still located around impeller and the gas slightly dispersed compared to the gas present when the impelled rotation is 200 rpm. At this point, loaded regime occurred as the flow transitions from flooded. Loaded pattern can be identified when the impeller speed is higher than impeller speed of flooded as well as lower than impeller speed of completely dispersed. Although the gas loaded at this regime is better able to distribute the gas radially, but the distribution of gas still poor due to the buoyant force being larger than drag force (Ford et al., 2008). The gas hold-up is decreasing as it pass along the x-axis plane at height, z = 0.8 cm and become constant with no present of gas. According to Calderbank (1958), the gas bubble size increase rapidly with the gas hold-up at high values of gas hold-up (< 40%), due to the bubble coalescence caused by the increasing proximity of the bubbles.

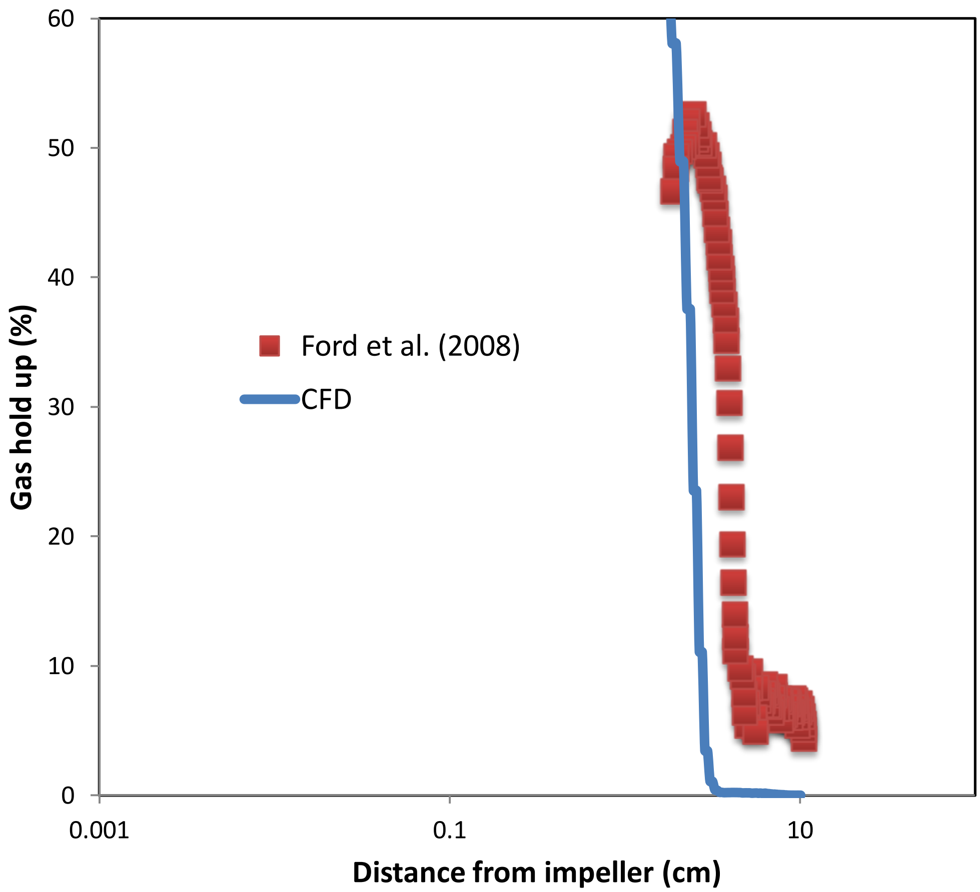

Figure 4.5: Local gas hold-up values along x-axis at height z = 0.8 cm for 700 rpm

Figure 4.5 shows the local gas hold-up at impeller speed 700 rpm. From this graph, the graph plotted represent the CFD simulation result has no agreement with the data of

Ford et al. (2008) due to the high percent of gas hold-up at point nearest to impeller hub with the percent up to 80%. Nevertheless, the pattern of the graph plotted is quite similar with the data plotted by Ford et al. (2008) as well as the trend of CFD simulation's graph plotted at **Figure 4.4.** Graph above shows the gas hold-up is decreasing as it pass along the x-axis plane at height, z = 0.8 cm and become constant with no present of gas started at point x = 3.26 cm from impeller. From **Figure 4.1**, power consumption indicates the flow at 700 rpm is completely dispersed. In comparison of present gas hold-up at three different impeller speeds; 200 rpm, 350 rpm, 700 rpm, it can be seen that the highest impeller speed; 700 rpm has the highest percentage of gas hold-up along the x-axis at z = 0.8 cm from the bottom of impeller. At lower impeller speeds, the impeller was unable to disperse the gas effectively, therefore outside impeller region has lower gas hold-up. Similar trends have been observed by Ford et al. (2008), although their data were obtained by experimental setup method using X-ray computed tomography (X-ray CT). The different of the percent of gas hold-up for all three different impeller speeds is due to a few factors which are the presence of cavities behind the impeller blade (refer **Figure 2.3**), pressure acting on the bubble and bubble rise velocity.

The contour of gas hold-up have been captured at z = 0.8 cm from bottom impeller. From **Figure 4.6**, the flow pattern can be seen and the prediction seems to be quite similar with Ford et al.'s (refer **Figure 2.3, Figure 2.4, Figure 2.5**) at Chapter 2. Nevertheless, still has discrepancy among both data. This is because, in this current study, a few things not are considered like the turbulence effect on the drag, shape of the bubble size, coalescence and non-coalescence bubble.

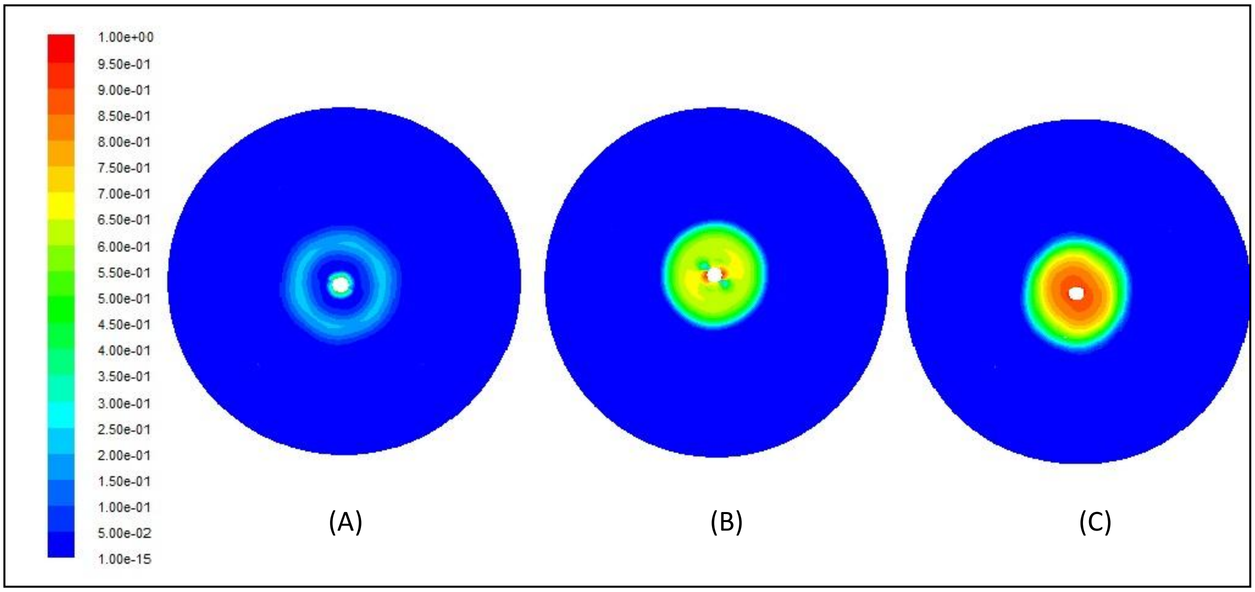

Figure 4.6: Prediction of gas hold-up along x-axis at height z = 0.8 cm from bottom of impeller for (A) 200 rpm, (B) 350 rpm and (C) 700 rpm

4.4.2 Average z-slice hold-up.

Figure 4.8, Figure 4.9, Figure 4.10 and **Figure 4.11** shows the average z-slice gas hold-up at constant gas flow rate 0.00015 m^3/s for the four different impeller speeds; 200 rpm, 350 rpm, 525 rpm and 700 rpm. The local time-averaged gas hold-up in each z-slice can be averaged to obtain an average slice hold-up. The time-averaged gas hold-up have been measured below impeller at point z = 4.75 cm until 12.75 cm whereby the impeller is located at 5.7 cm from the bottom of stirred tank. This measurement is important in order to determine the hold-up vertically simulate via CFD simulation in stirred tank. The impeller zone is covered at z = 4.75 cm to z = 6.65 cm whereby gas hold-up is increase dramatically for all four different impeller speeds. In comparison with Sun et al.'s results (**Figure 4.7**) at the same parameter study; to determine the gas hold up at the vertical plane, this work gave the results better prediction as shown in **Figure 4.8, Figure 4.9, Figure 4.10 and Figure 4.11.** There is an 'improvement' on the trend by comparing the simulation method to experimental method of Ford et al. (2008) for this study while Sun et al.'s prediction of simulation results have more divergence to their experiment results.

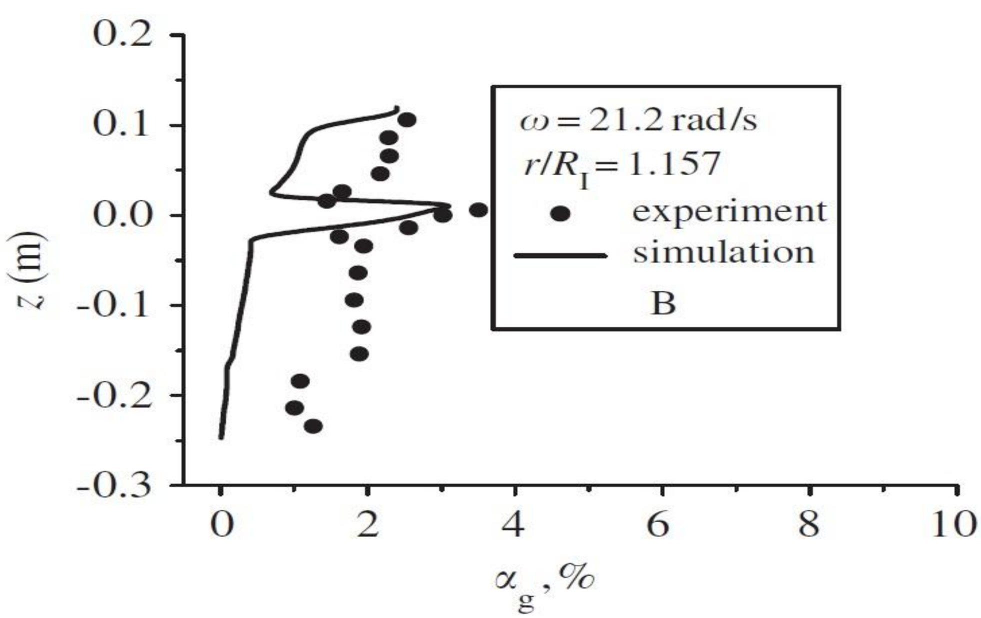

Figure 4.7: Comparison between the simulation and experiment with height vs. gas hold-up at ω = 21.2 rad/s. (Adapted from Sun et al., 2006)

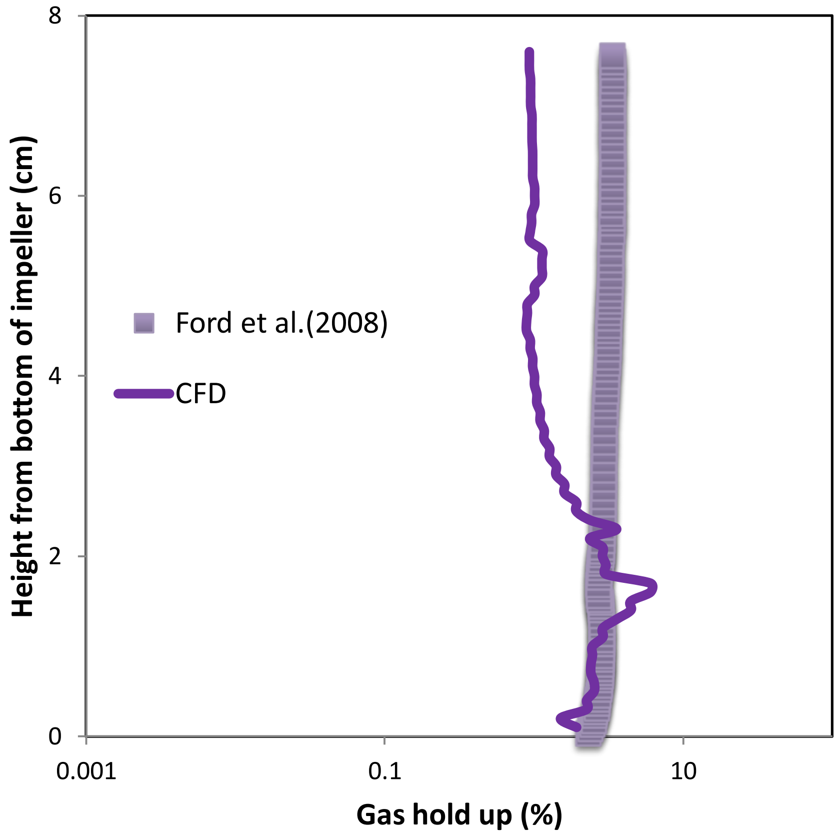

Figure 4.8: Average z-slice hold-up for 200 rpm

The average z-slice gas hold-up has been measured for 200 rpm as shown in **Figure 4.8**. The data reported by Ford et al. (2008) have been plotted to compare with this study to determine its achievable with Ford et al.'s data. From graph plotted by Ford et al.'s, the gas hold-up increase with the increasing of height due to low pressure acting on the bubble as the impeller speed is low, but compared to data plotted obtained in this study, at the region out of impeller zone, the gas hold-up is decreased as the height from the bottom of impeller is increased. This is due to the non-uniform distribution of gas within the tank. Since the data obtained from this study has discrepancy with the theory of fluid flow as well as the Ford et al.'s data, the improvement will be suggested at Chapter 5. According to Ford et al. (2008), at flooded regime, the impeller has a very little effect dispersing the gas that cause the lower pressure acting on the bubble, thus it cause the increasing of the bubble size and gas hold-up. Another one factor of the increasing of gas hold-up is there is an increase in drag that result the decreasing of bubble rise velocity.

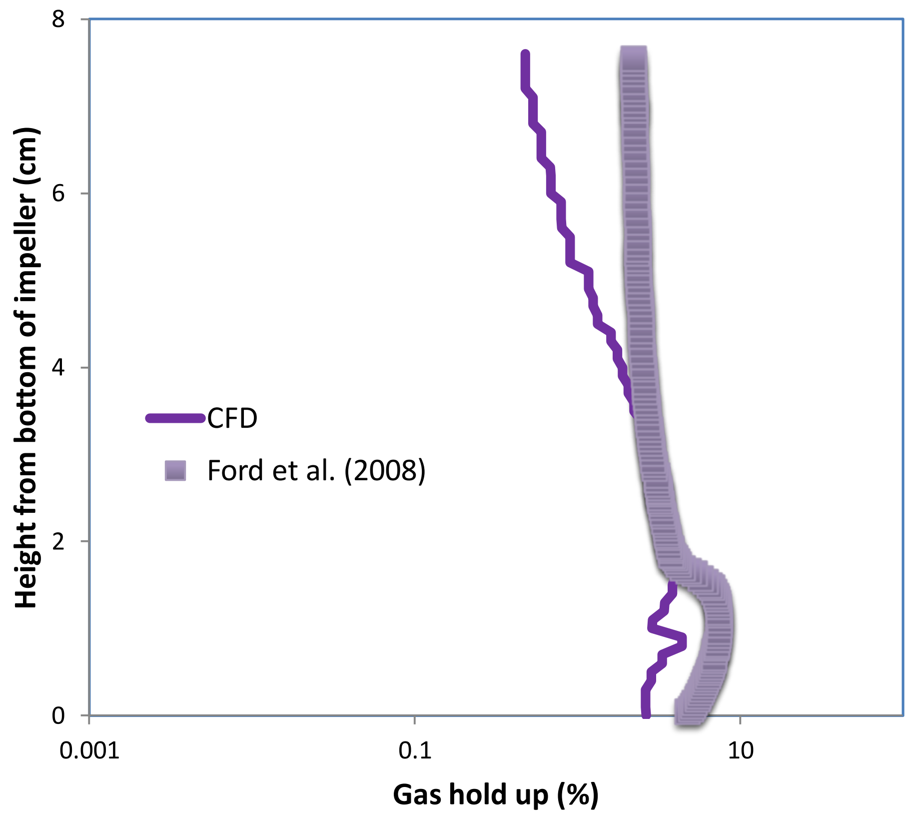

Figure 4.9: Average z-slice hold-up for 350 rpm

Figure 4.9 shows the time averaged gas hold-up at z-slice for 350 rpm where corresponds to the loaded regime as mentioned at power consumption (**Figure 4.1**) and local gas hold-up (**Figure 4.4**). From above graph, the result obtained via CFD simulation has a fair agreement with the data obtained by Ford et al. (2008). The gas hold-up is decreased as the height from the bottom of impeller is increased in the region out of impeller zone for both plotted graph; CFD and Ford et al. (2008). But little gas dispersed can be identified in this study due to very low gas hold-up as the height is increased compared to Ford et al.'s data. Besides that, another one trend (parabolic shape) that can be seen from **Figure 4.9** is the increasing of the gas hold-up as the height is increased at impeller zone for Ford et al.'s data and the result obtained from this study. According to Van't Riet and Smith, (1975) the parabolic shape at impeller zone is due to impeller capturing the gas.

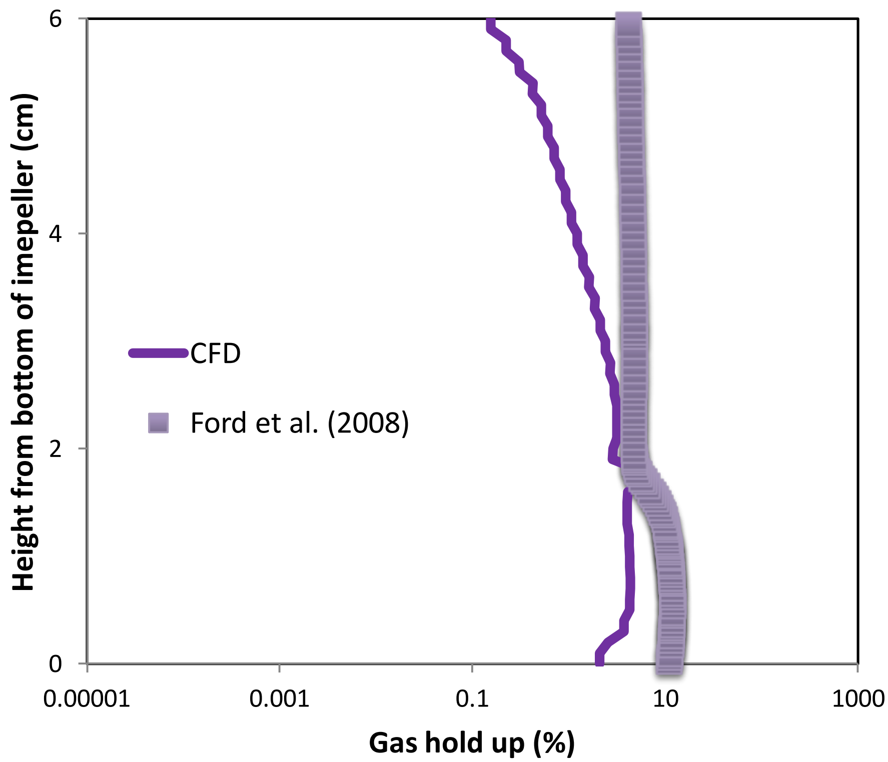

Figure 4.10: Average z-slice hold-up for 525 rpm

The same trend has been shown at **Figure 4.10** as **Figure 4.9**. The plotted graph at figure above is at impeller speed 525 rpm. At impeller zone, the gas hold-up is increased and decreased as the height is decreased due to the high pressure acting on the bubble that tend the gas to dispersed and go far away from the impeller compared to gas hold-up at 200 rpm and 350 rpm (**Figure 4.8, Figure 4.9**). Besides that, out of the impeller zone, the gas hold-up is decrease as the height from the bottom of stirred tank is increased. The same trend has been shown in this study with Ford et al.'s but unlike the percent of gas hold-up in Ford et al. (2008), the gas hold-up is started to be 0 at the height z = 6.2 cm from bottom of impeller while for the Ford et al. (2008), the gas hold-up is 4.1% at the same height.

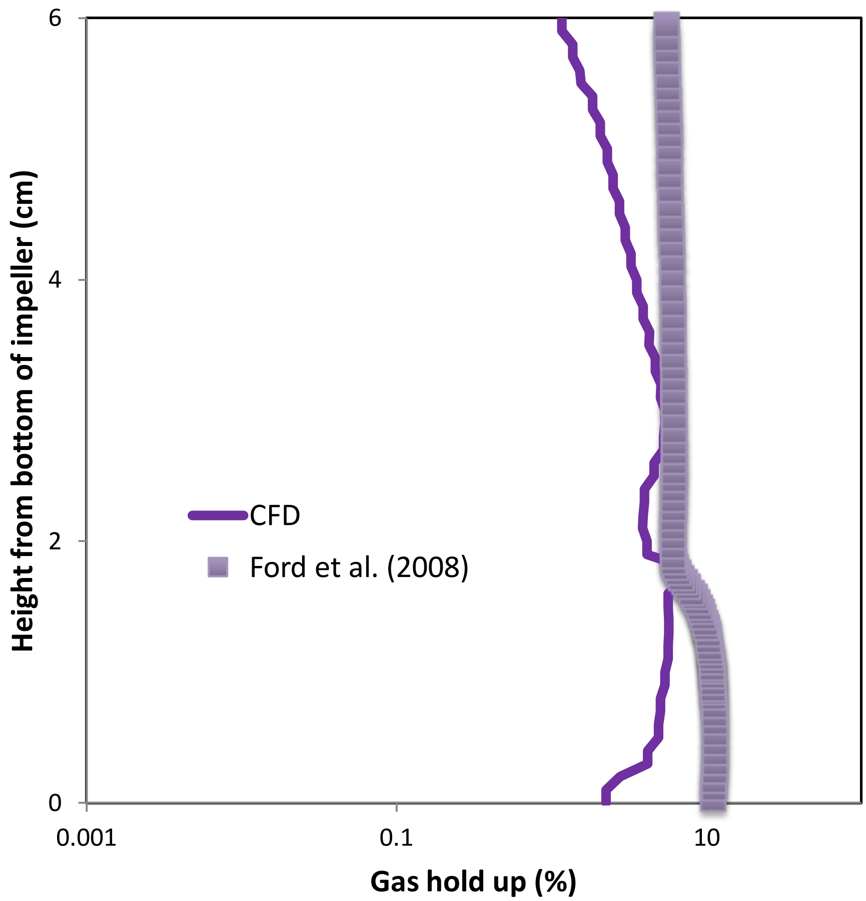

Figure 4.11: Average z-slice hold-up for 700 rpm

From **Figure 4.11**, the same trend and pattern at impeller zone and out of impeller zone have been shown by CFD study with Ford et al.'s at impeller speed 700 rpm. Based on the figure above, with the increasing of height from bottom of impeller, the gas hold-up is decreased at the impeller zone and decreased again linearly above the impeller zone. CFD result in gas hold-up has divergence with the data of Ford et al. (2008). This is because the various of bubble size has not been taken into account in Eulerian-Eulerian model and drag model. As what have been reported by Han et al. (2007), at lower velocity of bubble, the gas hold-up is high and more bubble at region close to shaft than near to the center axis under impeller. It is likely wrong in his prediction of gas hold-up because he implied the Discrete Particle Method which is often to be used for gas-solid hydrodynamics rather than gas-liquid because it employed Langragian method and Eulerian for quasi-fluid. For improvement, effect of bubble size on interaction should be involved. Same goes to this study, whereby the bubble size has not taken into consideration via CFD simulation.

Figure 4.12 shows the contour of gas hold-up along the z-slice at different impeller speed as well as different regime. From the figure, it can be seen the higher gas hold-up is near to the impeller as thee impeller speed is increase.

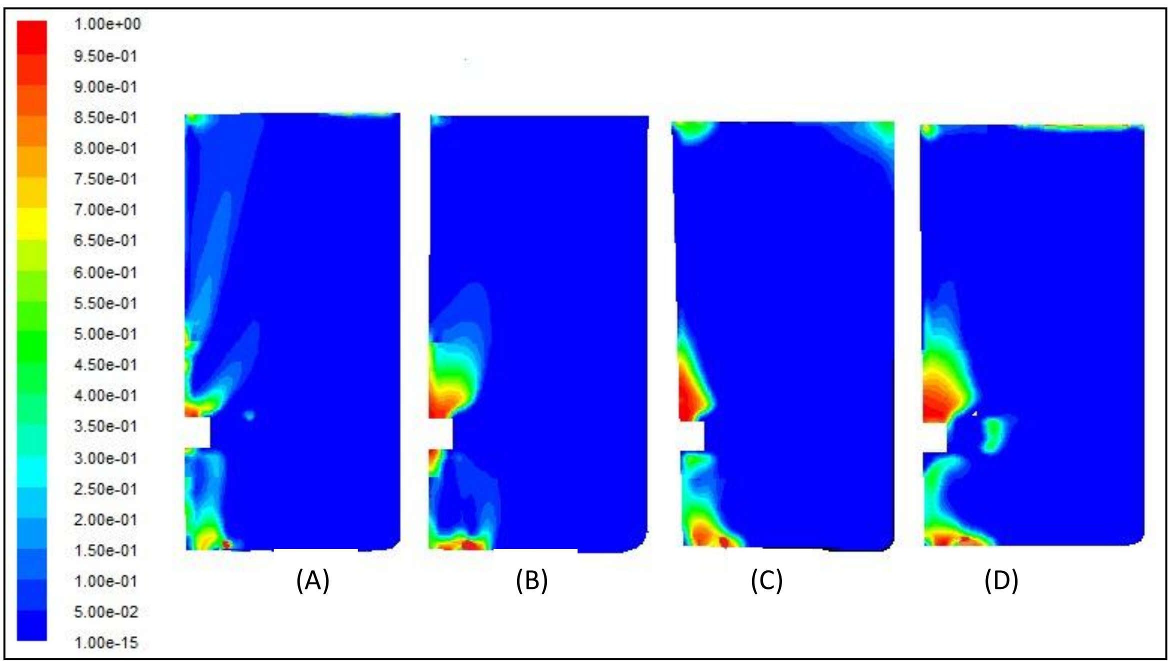

Figure 4.12: Prediction of average z-slice hold-up at (A) 200 rpm, (B) 350 rpm, (C) 525 rpm and (D) 700 rpm

4.5 Summary

In this study, the gas hold-up and power drop have been determine by using Computational Fluid Dynamics (CFD) simulation, Eulerian-Eulerian model, turbulence model, drag model and *Sauter* mean bubble size. Comparison between results by Ford et al. (2008) and this study have been analysed at different flow regime; flooding, loading and fully dispersed. As average, the data obtained from this study are not having good agreement with the data by Ford et al. (2008). This is due to unemployed some model by taking into account its turbulence effect on the drag, various sizes of bubble, drag model and coalescence of bubble as what have been proposed by Gimbun et al. (2009) by using Population Balance Model (PBM) and User Defined function (UDF).

CHAPTER 5

CONCLUSION

5.1 Conclusion

In this current study, computational fluid dynamic (CFD) was developed to investigate the fluid mechanics of multiphase flow (gas and liquid) in gas-liquid stirred tank. The aim of this study is to study the gas hold-up and power drop at various flow regime from flooding, loading to completely dispersion at gas-liquid stirred tank via CFD by comparing the result with published result of Ford et al. (2008).

Results from the aeration power number give a good agreement with the data prediction by Ford et al. (2008) except at impeller speed 700 rpm. This is because non-uniform bubble dispersion in gas-liquid stirred tank at high impeller speed. A good flow trend has been shown in predicting the local gas hold-up and average hold-up along the z-axis. However, there still has discrepancy in comparison with Ford et al.'s data. This is because, many things still not considered to have similar result as Ford et al.'s.

5.2 Recommendations

From this study, the results obtained for aeration power number and gas hold-up were expected to have similar result with Ford et al. (2008) at far lower cost of operating and require a shorter time to evaluate the performance of gas-liquid stirred tank. Therefore, this current study may be useful to eliminate the impeller flooding in gas-liquid stirred tank. In order to get better prediction, the combination of CFD, Population Balance Model

(PBM) proposed by Gimbun et al. (2009) for bubble breakage and coalescence and drag model by Ishii & Zuber (1979), Behzadi et al. (2004) and Schiller & Naumann (1935) for bubble size are recommended to be utilized in the future work.

.

REFERENCES

.

Ahmed S.U, Panneerselvam Ranganathan, Ashok Pandey, and Savithri Sivaraman, 2010 “Computational fluid dynamics modeling of gas dispersion in multi impeller bioreactor’’, *Journal of Bioscience and Bioengineering,* vol. 109, no. 6, pp. 588–597.

Bakker, A. & Van den Akker, H. 1994a, “Computational model for the gas-liquid flow in stirred reactors”, *Chemical Engineering Research & Design, Part A,* vol. 72, pp. 594-606.

Bakker, A. & Van den Akker, H. 1994, “Gas liquid contacting with Axial flow Impellers’’, *Chemical Engineering Research and Design,* vol. 72, no. A4, pp. 573-582.

Behzadi, A., Issa, R.I. & Rusche, H. 2004, “Modelling of dispersed bubble and droplet flow at high phase fractions”, *Chemical Engineering Science*, vol. 59, no. 4, pp. 759-770.

Bombac, A., Zun, I., 2006, “Individual impeller flooding in aerated vessel stirred by multiple-Rushton impeller”, *Chemical Engineer Journal,* vol. 116, pp. 85-95

Bouaifi, M., Hebrard, G., Bastoul, D. & Roustan, M. 2001, “Comparative study of gas hold-up, bubble size, interfacial area and mass transfer coefficients in stirred gas-liquid reactors and bubble columns”, *Chemical Engineering and Processing,* vol. 40, no. 2, pp. 97-111.

Brucato A., Grisa F., and Montante G., 1998, “Particle drag coefficients in turbulent fluids”, *Chemical Engineering Science*, Vol. 53, No. 18, pp. 3295-3314

Bukur D.B, Daly J.G, and Patel S.A, 1996, “Applicarion of gamma ray attenuation for measurement of gas hold up and flow regime transitions in bubble columns”, *Ind. Eng. Chem. Res*, vol. 35, pp. 70-80

Butcher, M. & Eagles, W. 2002, “Fluid mixing re-engineered”, *Chemical Engineer Journal*, no. 733, pp. 28-29.

Calderbank. 1958, “Physical rate process In industrial fermentation, Part 1: The Interfacial Area in Gas-Liquid Contacting with Mechanical Agitation”, *Institution of Chemical Engineers*

Deen, N.G., Solberg, T. & Hjertager, B.H. 2002, “Flow generated by an aerated Rushton impeller: Two-phase PIV experiments and numerical simulations”, *Canadian Journal of Chemical Engineering*, vol. 80, no. 4, pp. 638-652.

Derksen, J.J., Doelman, M.S. & Van den Akker, H. 1999, “Three-dimensional LDA measurements in the impeller region of a turbulently stirred tank”, *Experiments in Fluids* vol. 27, no. 6, pp. 522-532

Elgobashi S.E. and Abou-Arab T.W, 1983, “A two-equation turbulence model for two phase flows”, *Physics of Fluids*, vol.26, no.4, pp. 931-938

Fluent, (2005), Fluent 6.2 User Guide.

Fluent, (2006), Fluent 6.3 User Guide.

Ford, J.J., Heindel, T.J., Jensen, T.C. & Drake, J.B. 2008, “X-ray computed tomography of a gas-sparged stirred-tank reactor", *Chemical Engineering Science*, vol. 63, no. 8, pp. 2075-2085.

Gentrica C., D. Mignonb, J. Bousquetc, P.A. Tanguyd, 2005, “Comparison of mixing in two industrial gas–liquid reactors using CFD simulations’’, *Chemical Engineering Science* 60 (2005) 2253 – 2272.

Gimbun J., Rielly C.D, Nagy Z.K, 2009 “Mass transfer in gas-liquid stirred tanks agitated by Rushton turbine and CD-6 Impeller, *13th European Conference on Mixing London*

Han Luchang, *,L* IU Yuejin, and LUO He’an, 2007, “ Numerical Simulation of Gas Holdup Distribution in a Standard Rushton Stirred Tank Using Discrete Particle Method’’, *Chin. J. Chem. Eng.,* 15(6) 808-813.

Han Luchang, CAO Yang, WU Xuewen, BAI Ge, and LIU Yuejin, 2010, “The Effect of Eddy-bubble Interaction Model on the Turbulent Dispersion of Gas Bubbles in Stirred Tanks”, *Chinese Journal of Chemical Engineering*, 18(1) 27-33.

Heindel T.J, Gray J.N, Jensen T.C, 2008 “ An x-ray system for visualizing fluid flows”, *Flow Measurements and instrumentations 19,* pp. 67-78

Holland, F.A., Bragg, R., 1995. Fluid Flow for Chemical Engineers. Arnold, London, p. 173

Hughmark, G.A. 1980, “Power requirements and interfacial area in gas-liquid turbine agitated systems”, *Industrial & Engineering Chemistry, Process Design and Development,* vol. 19, no. 4, pp. 638-641.

Ishii, M. & Zuber, N. 1979, “Drag coefficient and relative velocity in bubbly, droplet or particulate flows”, *AICHE Journal,* vol. 25, no. 5, pp. 843-855.

Jose´ Manuel Go´mez, Domingo Cantero, 2002, “Kinetic study of biological ferrous sulphate oxidation by iron-oxidising bacteria in continuous stirred tank and packed bed bioreactors” , *Biotechnol. Adv. 39*, pp. 534-573.

Kamelia V.K. Boodhooa, Craig D. Cartwrighta, Marija Vicevica, Maria A. Prietob, Marta Tortajadac, 2004, “Development of a Higee bioreactor (HBR) for production of polyhydroxyalkanoate: Hydrodynamics, gas–liquid mass transfer and fermentation studies”, *Biochemical Engineering Journal 17*, pp. 129-136.

Kapic, A. & Heindel, T.J. 2006, “Correlating gas-liquid mass transfer in a stirred tank reactor’’, *Chemical Engineering Research and Design*, vol. 84, no. 3, pp. 239-245.

Khopkar, A., Aubin, J., Rubio-Atoche, C., Xuereb, C., Le Sauze, N., Bertrand, J., Ranade, V.V. 2004, “Flow generated by radial flow impellers: PIV measurements and CFD simulations”, *Int. J. Chem. Reactor Eng*. 2, A18.

Khopkar, A.R., Rammohan, A.R., Ranade, V.V. & Dudukovic, M.P. 2005b, “Gas–liquid flow generated by a Rushton turbine in stirred vessel: CARPT/CT measurements and CFD simulations”, *Chemical Engineering Science*, vol. 60, no. 8-9, pp. 2215-2229.

Khopkar, A.R., Aubin J., Xuereb C., Le Sauze N., Bertrand J. & Ranade, V.V. 2003, ‘’Gas-liquid flow generated by a pitched-blade turbine: Particle Image Velcimetry measurement and CFD simulation”, *Ind. Eng. Chem. Res.*, vol. 42, pp. 5318-5332

Kumar C.G, Hiroshi T., “Microbial Alkaline Proteases: From a Bioindustrial Viewpoint’’, *Biotechnol. Adv. 17* (1999), pp. 561–594.

Laakkonen, M., Moilanen, P. & Aittamaa, J. 2005c, “Local bubble size distributions in agitated vessels”, *Chemical Engineering Journal*, vol. 106, no. 2, pp. 133-143.

Lane G.L, Schwarz M.P, Evans G.M, 2002, “Predicted gas liquid flow in a mechanically stirred tank”, *Applied Mathematical Modelling* 26, pp. 223-235

Mudde R. and Siminin O., 1999, “Two and three-dimensional simulations of a bubble plume using a two fluid model”, *Chemical Engineering Science*, vol. 54, no.21, pp. 5061-5069

Murthy B.N., Kasundra R.B., Joshi J.B., “Hollow self-inducing impellers for gas–liquid–solid dispersion: Experimental and computational study’’, *Chemical Engineering Journal*, vol. 141, pp. 332–345.

Myers K.J., Fasano J.B., Bakker A. (1994), “Gas Dispersion Using Mixed High- Efficiency / Disc Impeller Systems”. *8th European Conference on Mixing, September 21-23, 1994, Cambridge, U.K.* IChemE Symposium Series No. 136, ISBN 0 85295 329 1, page 65-72.

Nienow, A.W., Wisdom D.J., Middleton, J.C., 1977, “The Effect of scale and geometry ion flooding, recirculation and power in gassed stirred vessels”, *In: Proceedings of the 2nd European Conference on Mixing, Cambridge, England,* pp. 1-16

Nienow, A. W., Warmoeskerken, M. M. C. G., Smith, J. M., & Konno, M. (1985), “On the flooding/loading transition and the complete dispersal condition in aerated vessels agitated by a Rushton-turbine*”, Proceedings of the Fifth European on mixing, Wurzburg, Germany*, pp. 143-153

Nienow, A.W., 1988, “Hydrodynamics of stirred bioreactors”, *Applied Mechanics Reviews* 51 (1), pp 3-32

Paglianti, A., Pintus, S. & Giona, M. 2000, “Time-series analysis approach for the identification of flooding/loading transition in gas-liquid stirred tank reactors”, *Chemical Engineering Science*, vol. 55, no. 23, pp. 5793-5802.

Perng, C.Y. and Murthy, J.Y., "A Moving Mesh Technique For the Simulation of Flow in Mixing Tanks", *AIChE Annual Meeting, Miami, FL*, paper 109b (1992).

Potumarthi R., Subhakar Ch., Jetty A., "Alkaline protease production by submerged fermentation in stirred tank reactor using *Bacillus licheniformis* NCIM-2042:Effect of aeration and agitation regimes", *Biochemical Engineering Journal* 34 (2007), pp. 185–192

Qingbai CAI and Gance DAI, 2010 " Flooding Characteristics of Hydrofoil Impeller in a Two- and Three-phase Stirred Tank'', *Chinese Journal of Chemical Engineering*, vol. 18, no.3, pp. 355—361

Ranade V.V., Gopal R. Kasat, Aniruddha B. Pandit, 2008, "CFD Simulation of Gas-Liquid Flows in a Reactor Stirred by Dual Rushton Turbines'', *International Journal of Chemical Reactor Engineering*, Vol. 6, article A60.

Rutherford, K., Mahmoudi, S.M.S., Lee, K.C. & Yianneskis, M. 1996, "Influence of Rushton impeller blade and disk thickness on the mixing characteristics of stirred vessels", *Chemical Engineering Research & Design,* vol. 74, pp. 369- 378.

Scargiali, F., D'Orazio, A., Grisafi, F. & Brucato, A. 2007, "Modelling and Simulation of Gas–Liquid Hydrodynamics in Mechanically Stirred Tanks", *Chemical Engineering Research and Design,* vol. 85, no. 5, pp. 637-646.

Schiller, L. & Naumann, L. 1935, "A drag coefficient correlation", *Z Ver Deutsch Ing*, vol. 77, p. 318.

Sun, H., Mao, Z. & Yu, G. 2006, "Experimental and numerical study of gas hold- up in surface aerated stirred tanks", *Chemical Engineering Science,* vol. 61, no. 12, pp. 4098-4110.

Tabor, G., A.D. Gosman and R.I. Issa, "Numerical Simulation of the Flow in a Mixing Vessel Stirred by a Rushton Turbine", *IChemE Symp.* Ser. 140, 25–34 (1996).

Taghavi Mahsa, Zadghaffari Ramin, Moghaddas Jafarsadegh, Moghaddas Yousef, 2010 "Experimental and CFD investigation of power consumption in a dual Rushton turbine stirred tank'', *Chemical Engineering Research and Design*-556.

Van 't Riet, K. & Smith, J.M. 1975, "Trailing vortex system produced by Rushton turbine agitators", *Chemical Engineering Science,* vol. 30, no. 9, pp. 1093- 1105.

Veera U.P, 2001, " Gamma ray tomography design for the measurement of hold-up profiles in two-phase bubble columns", *Journal of Chemical Engineering*, vol 81, pp. 251-260.

Warmoeskerken, M.M.C.G. & Smith, J.M. 1985, "Flooding of disc turbines in gas-liquid dispersions: a new description of the phenomenon", *Chemical Engineering Science,* vol. 40, no. 11, pp. 2063-2071.

Weijing Wang, Zai-Sha Mao, and Chao Yang, "Experimental and Numerical Investigation on Gas Holdup and Flooding in an Aerated Stirred Tank with Rushton Impeller'', *Ind. Eng. Chem. Res.* 2006, vol.45, pp.1141-1151.

Xiao Honghai and Takahashi Koji, "Gas Dispersion in Horizontal Non-Baffled Stirred Vessel with Rushton Turbine'', *Journal of Chemical Engineering of Japan*, vol.40, no.9, pp. 718-723, (2007).

Zhang Lifeng, "Mathematical simulation of fluid flow in gas-stirred liquid Systems'', *Modelling Simul. Mater. Sci. Eng.* 8 (2000), pp. 463–476.